

RANGE RESOLUTION IMPROVEMENT IN PASSIVE BISTATIC RADARS USING DECONVOLUTION

A THESIS SUBMITTED TO
THE GRADUATE SCHOOL OF ENGINEERING AND SCIENCE
OF BILKENT UNIVERSITY
IN PARTIAL FULFILLMENT OF THE REQUIREMENTS FOR
THE DEGREE OF
MASTER OF SCIENCE
IN
ELECTRICAL AND ELECTRONICS ENGINEERING

By
Musa Tunç Arslan
November, 2015

Range Resolution Improvement in Passive Bistatic Radars Using
Deconvolution

By Musa Tunç Arslan

November, 2015

We certify that we have read this thesis and that in our opinion it is fully adequate,
in scope and in quality, as a thesis for the degree of Master of Science.

Prof. Dr. Ahmet Enis Çetin(Advisor)

Prof. Dr. Hayrettin Köymen

Asst. Prof. Ali Ziya Alkar

Approved for the Graduate School of Engineering and Science:

Prof. Dr. Levent Onural
Director of the Graduate School

ABSTRACT

RANGE RESOLUTION IMPROVEMENT IN PASSIVE BISTATIC RADARS USING DECONVOLUTION

Musa Tunç Arslan

M.S. in Electrical and Electronics Engineering

Advisor: Prof. Dr. Ahmet Enis Çetin

November, 2015

Passive radar (PR) systems attract interests in radar community due to its lower cost and power consumption over conventional radars. However, one of the main disadvantages of a PR system is its low range resolution. The reason for this is, the range resolution depends on the bandwidth of the transmitted waveform and in a PR scenario, it is impossible to change transmitted waveform properties of a commercial broadcast. In this thesis, a post processing scheme is proposed to improve the range resolution of an FM broadcast based PR system. In the post processing scheme, the output of the ambiguity function is re-expressed as convolution of the autocorrelation of the transmitted signal and a channel impulse response. Therefore, it is shown that it is possible to use deconvolution methods to compute the channel impulse response using the output of the ambiguity function and the autocorrelation of the transmitted signal. Thus, using deconvolution to solve the channel impulse response provides an increase in the range resolution of the PR system. The method successfully increases the target separation distance and range resolution of a PR system using single FM channel signal. The conventional ambiguity function is able to separate two targets when the targets have about 17 km between each other where as the deconvolution based post processing method can decrease this to about 10 km. The deconvolution based post processing methods also decreases the side lobes around the target when the system uses multi channel FM signals. For a scenario in which three FM channels are employed, the highest side lobe is 1.2 dB below the main target peak and after deconvolution, this highest side lobe decreases to about 10 dB below the main target peak.

Keywords: passive radar, range resolution, deconvolution, target separation.

ÖZET

TERS EVRİŞİM KULLANARAK PASİF RADARLARDA MENZİL ÇÖZÜNÜRLÜĞÜ ARTIRMA

Musa Tunç Arslan

Elektrik ve Elektronik Mühendisliği, Yüksek Lisans

Tez Danışmanı: Prof. Dr. Ahmet Enis Çetin

Kasım, 2015

Pasif radar (PR) sistemleri, tipik olarak, ticari yayınlarG ile hedef tespiti yapan bi-statik radarlardır. Geleneksel radarlara göre düşük maliyetleri ve enerji harcamaları sebebiyle, PR sistemleri radar topluluğunun ilgisini çekmektedir. Fakat, bir PR sisteminin en büyük dezavantajı menzil çözünürlüğüdür, çünkü menzil çözünürlüğü yayın sinyalinin bant genişliğine bağlıdır ve ticari bir yayının dalga biçimini değiştirmek olanaksızdır. Bu tezde, FM yayın tabanlı bir PR sisteminin menzil çözünürlüğünü artırmak için, ters evrişim tabanlı bir sonradan işleme metodu sunulmaktadır. Belirsizlik denkleminin çıktısı, iletilen sinyalin özilintisinin bir kanal dürtü tepkisi ile evrişimi biçiminde yeniden yazılmaktadır. Dolayısıyla, iletilen sinyalin özilintisi ve belirsizlik denkleminin çıktısının ters evrişimi alınarak, kanal dürtü tepkisinin hesaplanabileceği gösterilmektedir. Tek FM kanallı PR sistemlerinde metod, başarılı bir şekilde hedeflerin ayrışma mesafesini düşürmekte ve menzil çözünürlüğünü artırmaktadır. Geleneksel belirsizlik denklemi, iki hedef arasındaki mesafe 17 km iken hedefleri ancak ayırabilmektedir, buna karşılık ters evrişim tabanlı sonradan işleme metodu, bu mesafeyi 10 km'ye kadar indirebilmektedir. Bununla birlikte, ters evrişim tabanlı metod, PR sistemi birden fazla kanallı FM sinyalleri kullandığında, hedef etrafında oluşan yan kulakların gücünü azaltmakta da kullanılabilir. Üç FM kanalı kullanan bir sinyal kullanıldığında, en güçlü yan kulak hedefe ait tepe noktasının 1,2 dB altında olacak kadar güçlü iken, ters evrişim sonunda bu seviye, 10 dB altında olacak kadar bastırılabilir.

Anahtar sözcükler: pasif radar, menzil çözünürlüğü, ters evrişim, hedef ayırma.

Acknowledgement

I would like to express my gratitudes to those who have helped me with completion of this thesis.

I owe particular thanks to Prof. Dr. A. Enis Çetin for giving me an opportunity of M.Sc. degree in Bilkent University, supporting me and showing me guidance in all of the hardships I have encountered throughout this thesis.

I would like to express my deepest appreciation to my family, my father Tunçay, mother Sevim and my beloved sister Gülce, for their endless, unconditional support and love in my whole life.

I would especially thank my colleague Devrim Şahin for being such a precious rubber duck for me, listening my thoughts, theories and providing me insight mixed with laughter at all times.

I thank my friends Oğuzhan Oğuz and Cem Doğru for their support and valuable friendship in my university years.

I would also like to thank Havelsan-EHSİM for providing their support during this thesis and TÜBİTAK for supporting this work under Grant Number 113A010.

Contents

- 1 Introduction** **1**
 - 1.1 A Brief History of Radars 2
 - 1.2 Passive Radars 5

- 2 The Ambiguity Function Based Target Detection and Passive Radar Signals** **6**
 - 2.1 Ambiguity Function 7
 - 2.1.1 FFT Based Computation of the Ambiguity Function . . . 9
 - 2.2 Passive Radar Signals 9
 - 2.2.1 FM Radio Broadcast 10
 - 2.2.2 Digital Audio and Video Broadcast 12
 - 2.2.3 GSM Telephone Signals 14
 - 2.2.4 Performance Summary 14

- 3 Range Resolution Problem in Passive Radars** **16**

3.1	Range Resolution in Radars	16
3.2	Range Resolution of Digital Waveforms	17
3.3	Range Resolution of Mixed Systems	19
3.4	Range Resolution Improvement Using Multichannel Signals	19
3.4.1	Doppler Ambiguity	20
3.4.2	Range Ambiguity	21
4	Range Resolution Improvement and Elimination of Side-lobes using Deconvolution	23
4.1	Ambiguity Function as a Convolution	23
4.2	Experiment Setup and Results of Deconvolution Algorithms	29
4.2.1	FM Radio Signals for Passive Radar in Computer Environ- ment	30
4.2.2	Passive Radar Receiver with Deconvolution Post Processing	33
4.2.3	Performance Measures	35
4.2.4	Simulation Results	37
5	Conclusion	51
A	Side-lobes and Multichannel Signals	56
B	DAMAS3 Deconvolution Algorithm	59

List of Figures

1.1	Mono-static radar geometry.	3
1.2	Bi-static radar geometry types.	4
2.1	Typical stereo FM baseband signal. \mathbf{L} is the left channel data and \mathbf{R} is the right channel data.	11
2.2	Typical spectrum of a complex baseband stereo FM signal. Inside the signal, there is Turkish folk music from Aşık Veysel.	12
2.3	2 DAB transmission frames.	14
3.1	Comparison of time-delay of auto-ambiguity functions of FM and DAB signals.	18
3.2	Comparison of single channel FM signal and 3 channel FM signal for radar purposes.	22
4.1	Several PSF examples used to solve deconvolution problem in FM based PR systems.	28
4.2	Template for stereophonic complex baseband FM signal generation.	30
4.3	Template for complex baseband multichannel FM signal generation.	31

4.4	Template for scenario generation.	32
4.5	Template for receiver block.	34
4.6	3-dB separation example with two targets at 10 and 26 km.	35
4.7	Several PSF examples used to solve deconvolution problem in FM based PR systems.	36
4.8	Results of the first experiment in Table 4.1.	38
4.9	Results of the first experiment with first target at 10 km and second target at 20 km.	39
4.10	Comparison of 3-dB separation performance of matched filter and deconvolution algorithms with respect to range.	40
4.11	Results of the second experiment with a single target at 10 km for $\Delta F = 50, 100$ kHz.	42
4.12	Results of the second experiment with a single target at 10 km for $\Delta F = 150, 200$ kHz.	43
4.13	Effect of ΔF on the side lobe amplitude.	44
4.14	Results of the third experiment with scenario in Table 4.2 and $\Delta F = 200$ kHz.	45
4.15	Results of the third experiment with scenario in Table 4.2 and $\Delta F = 150$ kHz.	46
4.16	Results of the third experiment with scenario in Table 4.2 and $\Delta F = 100$ kHz.	47
4.17	Results of the third experiment with scenario in Table 4.2 and $\Delta F = 50$ kHz.	48

4.18 Comparison of matched filter and deconvolution post processing algorithms in the side lobe sense.	49
---	----

List of Tables

2.1	Performance of main illuminators of opportunity [1].	15
4.1	Scenario for the first experiment on separation of targets.	37
4.2	Scenario for the first experiment on separation of targets.	44
4.3	Processing time of the deconvolution algorithms and the matched filter.	50

Chapter 1

Introduction

RADAR (**RA**dio **D**etection **ANd** **R**anging) is a system that uses electromagnetic waves to determine the range, speed and direction of an object. First system that can be called a radar is developed by Sir Robert Watson-Watt and his colleagues in 1936. In the so called Daventry Experiment, a BBC radio broadcast near Daventry county is used [2]. The broadcast had output power of 10 kW, wavelength of 49 cm, the beam was 30 degrees wide and 10 degrees elevation. A Hadley Page Bomber made several passes around the broadcast tower and several times, a clear returning signal was detected. This experiment showed that, it is possible to gather the reflections of an electromagnetic wave echoing from an object with a sensitive receiver. In addition to this, with signal processing methods, it is possible to detect the range, speed and direction of the object using the transmitted waveform and echo signal. Daventry Experiment was not only a radar, but also a passive radar, i.e. it used the already present BBC transmitter to detect the bomber [2].

In the conventional sense, a radar has a dedicated transmitter hardware, such that it transmits its own signal. This enables radar to change the transmitted waveform so that it can satisfy several properties, range resolution, Doppler resolution, detection range are some of these properties. Passive radar (PR) systems, also known as passive coherent location (PCL) or passive covert radar (PCR), on

the other hand does not have a transmitter, instead they use the already existing transmitters in the vicinity for object detection. These transmitters are called non-cooperative illuminators or illuminators of opportunity, and commonly consist of commercial transmitters such as FM radio, TV broadcasts, digital audio broadcast (DVB), or GSM telephone signals.

Some advantages of a PR system is that, it is low cost, transmitter is already built and broadcasting some sort of signal. Since the transmitter is already built by someone else, there is no need to make frequency allocations for the radar signal. In addition to this, it is very hard to find the location of the PR system, since the the system does not have a transmitter of its own and the receiver is mobile or easy to relocate in most of the cases.

The main disadvantage of a PR system is the inability to change the transmitted waveform to improve the radar performance and the transmit power. This causes low range resolution, low Doppler resolution, low overall detection range, need for more computational power due to dealing with signals that are not suitable for radars [1, 3, 4].

1.1 A Brief History of Radars

After the Daventry Experiment, Chain Home system developed by the same team and was the first fully functioning radar system as an early warning system before the Second World War against Germany. This radar had its own transmitters and was built in a bi-static fashion, in which the transmitter and receivers have separate hardware and located in different places [5]. This system was good enough to detect German aircraft masses over France as well due to high transmit power.

In response to this, Germany developed its own radar system, called Heidelberg-Gert device. This radar was a bi-static radar and used the British Chain Home system as its transmitter. In fact, Daventry Experiment showed

that a radar does not necessarily need to generate the transmitted waveform itself, it can use an existing source and use it to detect the aircrafts. German Heidelberg-Gert device was a fully functioning PR system and it had all the covert advantages of such a system. By the end of the Second World War, it was certain that radars were extremely useful as an early warning device.

After the Second World War, British Chain Home system was updated several times against Russians during the Cold War. Several other systems from Russia and USA were built in order to detect a nuclear missile launch or bomber attack.

Another application of radar during the Cold War was for scientific purposes. In 1961, at NASA's Goldstone Observatory, terrestrial mapping of Venus was conducted as an experiment using radars. In 1965, in the Bell Labs, cosmic background radiation was observed by chance during a radar calibration.

Radar systems increased in popularity both as a defense system and for scientific purposes. In the early radar applications, receiver and transmitter hardware were separate due to lower cost, fast and cheap switches were not available yet. Radar systems are divided in to three categories based on the location of transmitters and receivers. When the transmitter and receiver are parts of the same system it is called the mono-static geometry. A mono-static radar has the geometry in the Fig. 1.1.

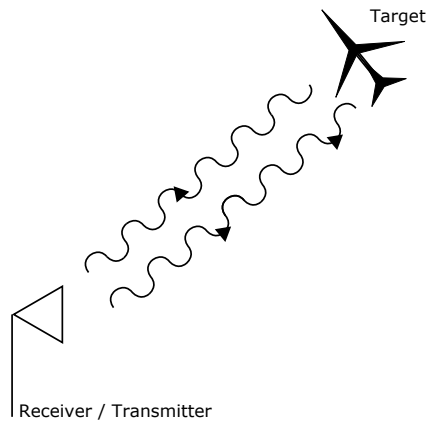
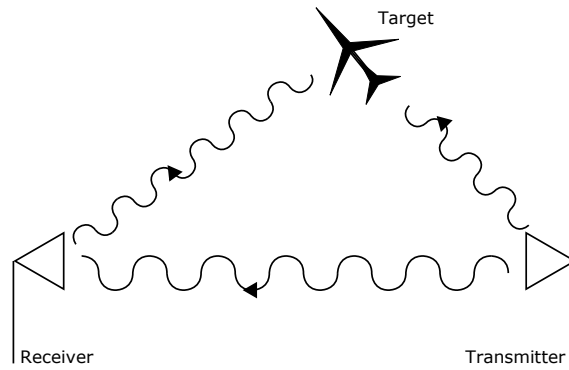
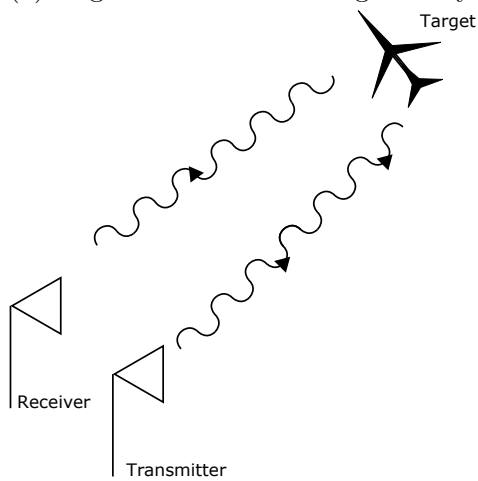


Figure 1.1: Mono-static radar geometry.

If the receiver and transmitter are in separate locations far from each other, such systems are called bi-static. Bi-static radars are more robust against radar cross section due to geometrical effects. However, the system has more complex geometry. Possible bi-static radar has the transmitter and receiver deployments shown in Fig. 1.2. The geometry in Fig. 1.2b enables the radar to use a simplified geometry in exchange of the benefits of the regular bi-static geometry.



(a) Regular bi-static radar geometry.



(b) Simplified bi-static radar geometry.

Figure 1.2: Bi-static radar geometry types.

1.2 Passive Radars

PR (passive radar) systems are bi-static radars in which the transmitter is most typically a commercial broadcast, such as radio or TV. This definition also makes the Daventry Experiment a PR system as well. Dependency on the commercial broadcast limits the performance of a PR system in several departments, since the commercial broadcast antennas are built for purposes other than target detection. These limitations most generally revolve around the range resolution and detection range. Range resolution is inversely proportional with the baseband bandwidth of the transmitted signal and typically commercial broadcasts such as FM radio or digital radio have low baseband bandwidth. In addition to this, commercial broadcast signals are not specifically designed to fulfill certain radar needs as well. Thus, the range resolution is a major issue in PR systems.

The aim of this thesis is to give an insight to the range resolution problem in PR systems and enhance the range resolution of PR systems using a post processing method based on deconvolution. In the Chapter 2, typical PR system transmit signals and detection of targets inside these signals are explained. In Chapter 3, the range resolution problem in PR systems and literature in this subject is covered. In Chapter 4, solution to range resolution in PR systems using a deconvolution based post processing method, the PR system of concern, performance measures and experimental results are presented.

Chapter 2

The Ambiguity Function Based Target Detection and Passive Radar Signals

Radars are divided in to three categories according to the transmitter and receiver hardware location. In the mono-static radar case, transmitter and receiver are co-sited. When the transmitter and receiver systems are not co-sited, the system is called bi-static radars. Multi-static radars on the other hand use several transmitters and each receiver-transmitter pair can be either mono-static or bi-static [6, 7]. Mono-static radars have the advantage of simpler radar geometry compared to bi-static and multi-static cases. However, bi-static radars have better detection performance when the target of concern have lower radar cross-section head on or against stealth aircrafts in exchange for more complex radar geometry [6, 8].

2.1 Ambiguity Function

The radar ambiguity function is the main tool for range and Doppler estimation in both mono-static and bi-static radars [3, 4, 6, 7, 9]. The output of the ambiguity function is the output of the matched filter with time delay τ and Doppler shift f . When an object in the air has a distance corresponding to a time delay of τ_p time delay and a speed corresponding to a Doppler shift of f_p , the ambiguity function “matches” the transmitted and received waveforms and generates a peak. Considering the bi-static case for the PR system, transmitted waveform is gathered from a reference antenna and can be written as follows in the continuous time domain:

$$s_{ref}(t) = s(t - \tau_r), \quad (2.1)$$

where $s(t)$ is the transmitted waveform and τ_r is the time delay of the transmitted waveform to reach the receiver antenna due to the distance between two. The reference signal is denoted by $s_{ref}(t)$ in this thesis. In conventional radars the transmitted waveform is known a priori and is generated by the radar system itself, τ_r is simply taken as zero and the ambiguity function equation is further simplified. The transmitted signal also echoes from several objects around it, e.g. planes, cars, clouds, bird flocks and hills, reaches the radar and is gathered from a surveillance antenna. This surveillance signal is expressed as follows in the continuous time domain:

$$s_{surv}(t) = \sum_{p=1}^P a_p s(t - \tau_p) e^{j2\pi f_p t}, \quad (2.2)$$

where P is the total number of reflecting objects around the radar, a_p is the attenuation of the signal that is echoing from the p^{th} target, τ_p is the time delay of the signal that is echoing from the p^{th} target and f_p is the Doppler shift of the signal that is echoing from the p^{th} target.

The continuous-time domain ambiguity function that uses Eq. 2.1 and 2.2 is

defined as follows:

$$\xi(f, \tau) = \int_{-\infty}^{\infty} s_{surv}(t) s_{ref}(t - \tau)^* e^{-j2\pi ft} dt \quad (2.3)$$

where f is the Doppler shift index representing the speed and τ is the time shift index representing the range. Substituting Eq. 2.1 and 2.2 into 2.3 we obtain:

$$\xi(f, \tau) = \int_{-\infty}^{\infty} \left(\sum_{p=1}^P a_p s(t - \tau_p) e^{j2\pi f_p t} \right) \left(s(t - \tau_r - \tau) \right)^* e^{-j2\pi ft} dt \quad (2.4)$$

We can rearrange the terms as follows:

$$\xi(f, \tau) = \int_{-\infty}^{\infty} \left(\sum_{p=1}^P a_p s(t - \tau_p) e^{j2\pi(f_p - f)t} \right) \left(s^*(t - \tau_r - \tau) \right) dt \quad (2.5)$$

In the case of $f = f_p$ exponential term will be equal to 1 and we can take the inner sum to outside. Then we make the Doppler shift f_p a subscript, the ambiguity function will have the following form:

$$\xi_{f_p}(\tau) = \sum_{p=1}^P a_p \left(\int_{-\infty}^{\infty} s(t - \tau_p) s^*(t - \tau_r - \tau) dt \right) \quad (2.6)$$

The inner integral is the continuous time auto correlation of the transmitted signal and will give a global peak when the signal time delays are matched, i.e., $\tau = \tau_p - \tau_r$. Hence the inner integral is also called “the matched filter” and with this approach, ambiguity function finds the target time delays and Doppler shifts in a radar scenario. Most bi-static radar systems and the algorithms developed in this thesis take advantage of Eq. 2.6. Ambiguity function can also be calculated using a faster, FFT based approach.

2.1.1 FFT Based Computation of the Ambiguity Function

Eq. 2.3 can be reexpressed in discrete time domain as follows.

$$E[\zeta, k] = \sum_{n=0}^{N-1} s_{surv}[n]s_{ref}^*[n - \zeta]e^{-j2\pi kn/N}. \quad (2.7)$$

where ζ is the range bin representing the sample time delay and k is the Doppler bin representing the sampled Doppler shift. Eq. 2.7 can be computed using the FFT algorithm. For each range bin ζ , the FFT based method is executed as follows:

Algorithm 1: FFT based calculation of ambiguity function.

Input: $s_{ref}[n]$, $s_{surv}[n]$

Output: $E[\zeta, k]$

- 1 Rotate surveillance signal $s_{ref}[n]$ by a range bin, ζ ,
 - 2 Element-wise multiply $s_{ref}[n - \zeta]$ and reference signal $s_{surv}[n]$,
 - 3 Calculate the N-point FFT of $s_{surv}[n]s_{ref}^*[n]$,
 - 4 Repeat from (1) until all range bins, ζ , are covered.
-

In this method, each FFT coefficient will correspond to a Doppler bin and each rotation amount ζ will correspond to a range bin which is also equal to the range resolution of the PR system. In the next section, common illuminators of opportunity signals, their mathematical background and range resolution performance in a PR system are examined.

2.2 Passive Radar Signals

PR systems exploit illuminators of opportunity. These illuminators are most commonly, FM radio, digital audio broadcast (DAB), digital video broadcast (DVB), GSM telephone and wi-fi signals. Naturally, different broadcast types have different radar performance and have their own trade-offs.

2.2.1 FM Radio Broadcast

FM radio broadcast, invented in 1930s, is a very high frequency (VHF) frequency modulation (FM) scheme to provide high-fidelity sound to listeners. In most European countries, DAB systems have started to replace FM broadcasts, however, in the developing countries it is still used and will remain to be used in the near future. The freq. band of the FM broadcast is between 87.5 to 108 MHz. In Turkey, each adjacent channel is separated by 200 kHz and the frequency deviation is ± 75 kHz, which results in a maximum of 150 kHz bandwidth for a FM channel [10]. The overall bandwidth of the FM channel is highly dependent on the transmitted message signal, i.e. a calm conversation causes significantly less overall bandwidth when compared to the rock music [3]. This high variation significantly changes the overall range resolution of the FM based PR system from 1.5 km to 15 km [1, 3, 9, 4].

The stereo FM signal is the standard FM signal generation technique. The left and right channel information are the main data to be sent and sometimes a radio data system (RDS) is also used. RDS is a simple, low bandwidth (≈ 2 kHz), low throughput (≈ 1187 bps) system which might include, weather information, FM radio channel information or other text based informations [10]. RDS is generally not employed in Turkey.

A pilot tone of 19 kHz is employed to distribute the sound and RDS data inside the FM channel. Baseband consists of summation of left and right channels, at the first harmonic a simple cosine signal carries the pilot tone, at the second harmonic of the pilot tone (38 kHz) subtraction of left and right channels are carried and at the third harmonic of the pilot tone (57 kHz) the RDS is employed [10]. The distribution of the stereo FM signal in the frequency domain is shown in Fig. 2.1.

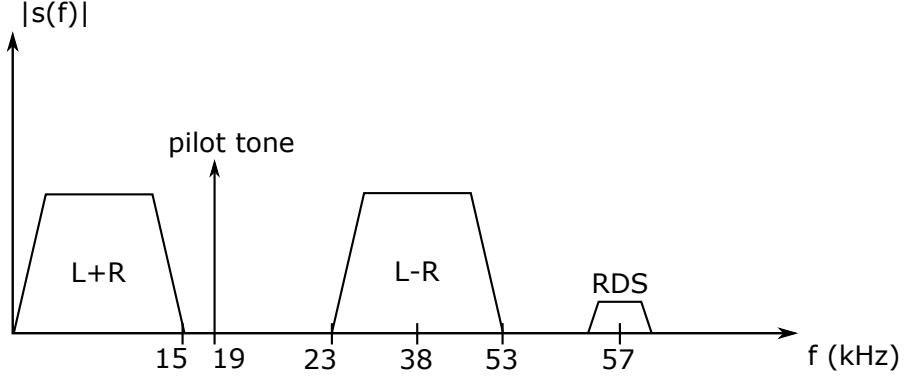


Figure 2.1: Typical stereo FM baseband signal. \mathbf{L} is the left channel data and \mathbf{R} is the right channel data.

The baseband stereo FM signal is generated as follows:

$$m(t) = \frac{L(t) + R(t)}{2} + \frac{L(t) - R(t)}{2} \cos(2\pi 2f_{pilot}t) + RDS(t) \cos(2\pi 3f_{pilot}t) + \cos(2\pi f_{pilot}t), \quad (2.8)$$

where $m(t)$ is called the “message signal” which contains the data to be transmitted, $L(t)$ is the left channel data, $R(t)$ is the right channel data, $RDS(t)$ is the RDS data and $f_{pilot} = 19$ kHz is the pilot tone [10, 11]. Then this message signal $m(t)$ is frequency modulated as follows:

$$s(t) = \cos\left(2\pi k_f \int_{-\infty}^{\infty} m(t) dt\right) + j \sin\left(2\pi k_f \int_{-\infty}^{\infty} m(t) dt\right). \quad (2.9)$$

In Eq. 2.9, $s(t)$ is the complex baseband stereo FM signal with modulation index k_f . During the target range and Doppler estimation, this complex baseband signal is used by the radar. An example spectrum of a complex baseband stereo FM signal is shown in Fig. 2.2. In this signal the maximum frequency deviation is ± 75 kHz and there is no RDS.

It is reported that FM broadcast based PR systems can detect and track targets at up to 150 km away from the transmitter and bistatic ranges up to 300 km [4].

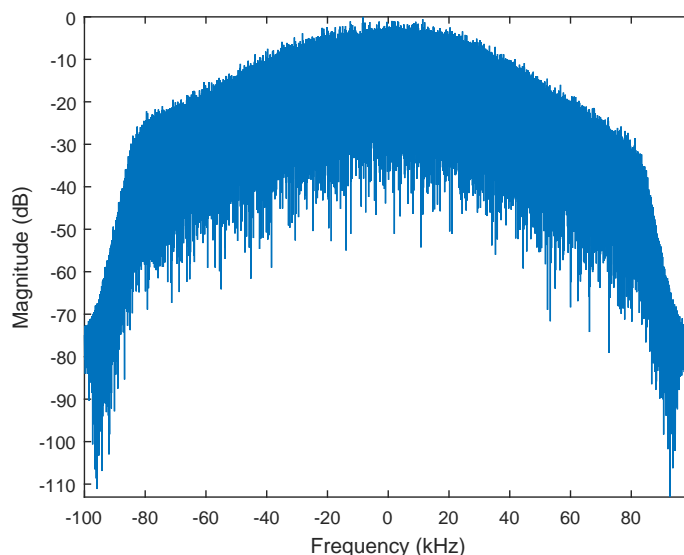


Figure 2.2: Typical spectrum of a complex baseband stereo FM signal. Inside the signal, there is Turkish folk music from Aşık Veysel.

2.2.2 Digital Audio and Video Broadcast

First Digital Audio Broadcast (DAB) system was introduced in 1995 by the Norwegian Broadcasting Corporation. DAB, Digital Video Broadcast (DVB), and many more digital modulation based systems use the orthogonal frequency division multiplexing (OFDM) scheme to transmit the digital data. DAB offers more radio channels, better sound quality due to high bit rate and is more robust to multipath fading and noise. In the DAB standards, bandwidth of the baseband DAB signal is determined as 1.536 MHz. DAB based PR systems offer better range resolution due to the high bandwidth and impulse shaped output at the matched filter due to their noise like spectrum, a byproduct of the OFDM scheme. However, compared to the FM radio, overall output power of the DAB signal is significantly low, between 1 to 10 kW, which results in lower detection range compared to the FM based PR systems.

Mode 1 DAB signals, which is the DAB radio, are divided in to 1.246 milliseconds (ms) blocks and each block consists of 1536 sub-carriers which are modulated

with differential quadrature phase shift keying (D-QPSK) scheme. Since all adjacent sub-carriers are 1 kHz apart from each other, the baseband DAB signal has 1.536 MHz bandwidth [12]. A 1.246 ms OFDM block is generated using the following equation:

$$s_i(t) = \sum_{n=-N/2}^{N/2-1} x_i[n] e^{j2\pi n \Delta f t} q(t), \quad (2.10)$$

where N is the sub-carrier number and is equal to 1536, $x_i[n]$ is the D-QPSK symbol to be modulated with the sub-carrier, $\Delta f = 1$ kHz, and $q(t)$ is a square signal defined as follows:

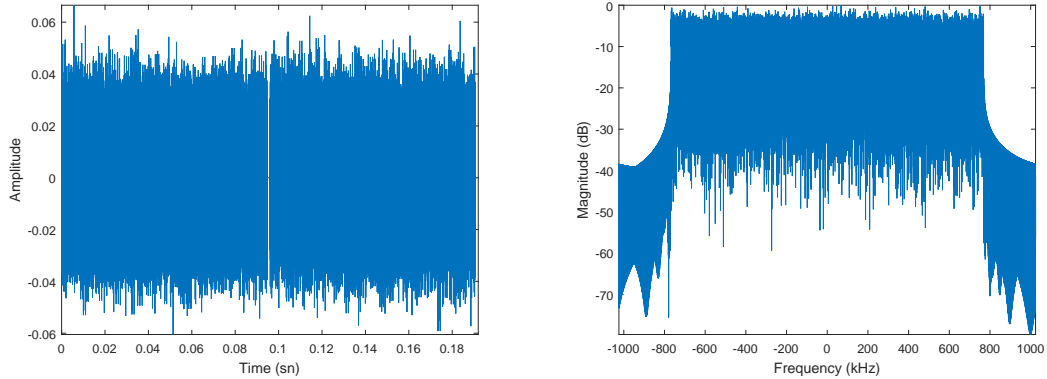
$$q(t) = \begin{cases} 1, & t \in [-T_{cp} \ T] \\ 0, & \textit{otherwise} \end{cases} \quad (2.11)$$

where T_{cp} is the cyclic prefix time and is equal to 0.246 ms, T is equal to 1 ms. Each block created with 2.10 is then concatenated and the complex baseband transmit signal is generated as follows [12]:

$$s(t) = \sum_{i=-\infty}^{\infty} s_i(t - iT'), \quad (2.12)$$

where $T' = T_{cp} + T = 1.246$ ms. Concatenation of 76 OFDM symbols generates a 96 ms signal called transmission frame. A 1.297 ms second null symbol follows each transmission frame, creating a block of zeros between each transmission frame. Null symbol indicates a transmission frame is finished and a new one is coming, in the DAB receiver [12]. Real part of a time domain DAB signal with 2 transmission frames is in Fig. 2.3a. Clearly from Fig. 2.3b, DAB signals have a bandwidth of 1.536 MHz, which results in about 200 meters range resolution, 8 times better than the FM broadcast case. However, DAB systems suffer from the overall detection range due to transmitter characteristics and use of single frequency networks (SFN), up to 60 kms [1, 13], which is about one third of FM based PR system capability.

DVB signal is generated with the same OFDM approach, the signal bandwidth is higher, 8 MHz, and the overall range resolution is significantly better when



(a) Real part of the time domain of a DAB signal with 2 transmission frames. (b) Spectrum of the DAB signal with 2 transmission frames in Fig 2.3a.

Figure 2.3: 2 DAB transmission frames.

compared to both DAB and FM cases. However, similar with the DAB, DVB transmitter characteristics and use of SFN structure, the overall detection range is limited [1, 14].

2.2.3 GSM Telephone Signals

GSM base stations provide the lowest overall detection range when compared to FM radio, DAB and DVB. This is due to low transmit power mainly. However, GSM base stations are built in a tight grid therefore can be useful when tracking a target efficiently while it is passing through several base station coverage areas. Thus, GSM based PR systems can be beneficial for vehicle traffic tracking. However, in an aircraft detection scenario, GSM signals are not useful [1].

2.2.4 Performance Summary

Performance of FM radio, DAB, DVB and GSM telephone signals can be summarized in the following Table 2.1.

The highest transmit power belongs to the FM radio and it is reported that FM

Table 2.1: Performance of main illuminators of opportunity [1].

Broadcast Type	Carrier frequency	Typical bandwidth	$P_t G_t$	Power density
FM radio	88-108 MHz	FM, max 150 kHz	250 kW	100 km, -57 dBW/m^2
DAB	≈ 220 MHz	OFDM, 1.536 MHz	10 kW	100 km, -71 dBW/m^2
DVB	≈ 750 MHz	OFDM, 2, 4, 6, 8 MHz	8 kW	100 km, -72 dBW/m^2
GSM	$\approx 900, 1800$ MHz	GMSK, FDM/TDMA/FDD 200 kHz	100 W	100 km, -81 dBW/m^2
GSM-3G	≈ 2 GHz	CDMA, 5 MHz	100 W	100 km, -81 dBW/m^2

radio is capable to detect targets at 300 km bi-static range. DAB and DVB has similar transmit powers and thus similar detection range, however, DVB provides higher bandwidth, which is beneficial in the range resolution sense. However, DVB transmitters are not as common as DAB which limits the overall coverage and freedom of the system. GSM telephone signals have the lowest transmit power but also have the best urban coverage. With the use of several GSM base stations, it is possible to track a target across several base stations. However, very low detection range limits the usefulness of GSM base stations for air traffic detection practically impossible [1].

One main advantage of FM radio, is the high transmit power. Even though FM, DAB, DVB transmitters have similar antennas, omni directional and set up on high masts, relatively high transmit power of FM radio makes it a better candidate for long range detection compared to digital systems. One major disadvantage of FM based PR system is the low range resolution due to low baseband signal bandwidth. In this thesis, FM radio broadcasts are considered as illuminator of opportunity due to longer detection range and low range resolution.

Chapter 3

Range Resolution Problem in Passive Radars

One main disadvantage of PR systems is the low range resolution, due to inability of changing the properties of transmitted waveform. Range resolution problem in PR systems is not well studied [15, 8, 16]. In general, the waveform of consideration is completely changed to a more suitable one for better range resolution. In this chapter, literature on subject of the range resolution problem in passive radars is reviewed.

3.1 Range Resolution in Radars

In a radar system, range resolution is defined using the following equation [6]:

$$\Delta R = \frac{c}{2\beta}, \quad (3.1)$$

where c is the speed of light and β is the bandwidth of the signal used in the radar system. In addition to this, the range resolution is further limited by the main lobe of the autocorrelation function of the transmitted signal [17]. In order

to narrow down the main lobe of the autocorrelation function, the transmitted waveform has to have noise-like frequency domain properties.

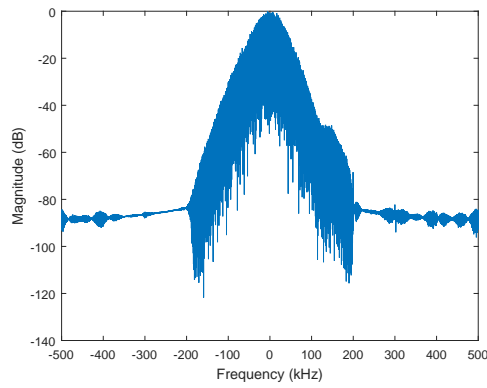
In a conventional radar, β can be changed to match the needed performance of the system and the transmitted signal can be engineered such that it is noise-like in the frequency domain. However, in the case of passive radars, this is not possible. The waveforms are already in the air, being broadcast from commercial antennas. Thus, one of the main disadvantages of a PR system is the low range resolution.

3.2 Range Resolution of Digital Waveforms

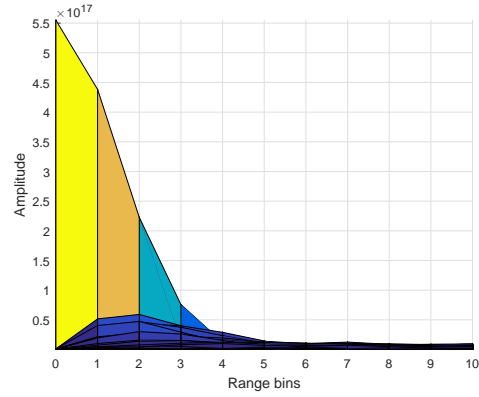
The most straightforward method to increase the range resolution is to use an illuminator of opportunity that has a baseband signal with higher bandwidth, i.e., DAB or DVB. An FM channel has a maximum of 150 kHz bandwidth and is highly dependent on the message signal [3], a DAB signal, on the other hand, has constant 1.536 MHz bandwidth, which corresponds to about 200 meters range resolution, seven times better than an FM based PR can provide.

DVB signals have constant 2, 4, 6 or 8 MHz bandwidths depending on the mode of the transmitter, which is even higher than DAB. As a result it is possible to have a 40 meter range resolution. Digital waveforms such as DAB or DVB, has a noise-like frequency domain shape, which is further beneficial since the main lobe of the autocorrelation function will be narrower.

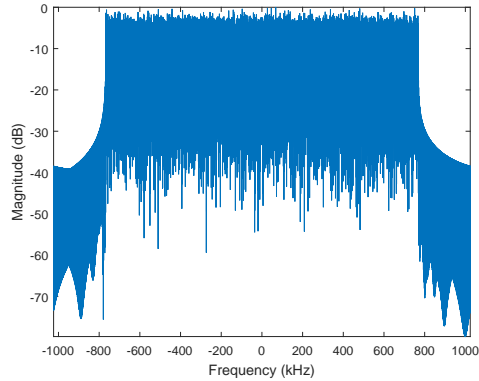
Effect of noise-like frequency domain shape on the main lobe of the autocorrelation function is illustrated in Fig. 3.1. In the FM case, the main lobe of the auto-ambiguity function spreads as far as to the 4th range bin, which approximately equals to 12.5 km in this case. In the DAB case, the peak is as wide as one range bin due to the noise-like frequency domain structure. Theoretically, auto-ambiguity results of any radar signal should provide a sharp peak, i.e. a peak as



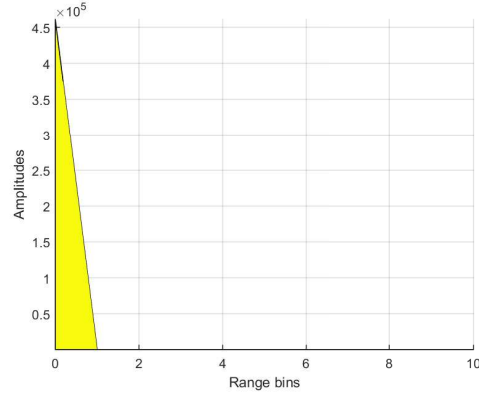
(a) Spectrum of a complex baseband FM signal.



(b) Auto-ambiguity function results of the signal in Fig. 3.1a.



(c) Spectrum of a complex baseband DAB signal.



(d) Auto-ambiguity function results of the signal in Fig. 3.1c.

Figure 3.1: Comparison of time-delay of auto-ambiguity functions of FM and DAB signals.

wide as one range bin, hence the range resolution is achieved. However, the frequency domain structure of the FM signal prevents this and the auto-ambiguity function widens, decreasing the range resolution performance further.

A brief glimpse to the subject suggest that using DVB or DAB signals for the PR system is the logical approach. However, DAB and DVB have their own drawbacks, such as overall low detection range compared to FM broadcast due to the low radiated power and other system properties [1]. Ideally, a radar should both have good range resolution and good overall detection range. DAB or DVB broadcasts satisfy the range resolution criterion however lack the detection range capabilities of a FM based PR system.

3.3 Range Resolution of Mixed Systems

In order to deal with the low range resolution of FM based PR systems and the low maximum detection range of DAB or DVB based PR systems, a mixed type system is proposed in [18, 16]. This system uses FM broadcast for high maximum detection range, DAB and DVB broadcasts for high range resolution, in order to benefit from the advantages of all of the different broadcast types. The system is divided into several subsystems and each subsystem uses a different broadcast type for detection. However, the subsystem structure preserves all the drawbacks of the broadcast type, such as, the FM subsystem still has very low range resolution and DAB or DVB subsystems still have low maximum detection range compared to FM. At further ranges, the system uses only FM broadcast for detection and has very low range resolution. The targets are identified as a cluster and tracked.

At closer ranges, DVB and DAB subsystems are used for increased range resolution and clusters are further dissolved in to separate targets. The target clusters that are being tracked by FM subsystem can now be identified and separated from each other [18, 16]. This approach is useful, but does not increase the overall performance of the PR system in longer ranges, does not improve the range resolution of FM subsystems at all and does not increase the overall detection range of DAB or DVB subsystems.

3.4 Range Resolution Improvement Using Multichannel Signals

Since several FM, DAB or DVB channels are all in the air at the same time, it is possible to use consecutive channels with a high bandwidth receiver in the radar. The overall bandwidth will increase due to using several consecutive channels, and the range resolution will improve. This approach is first suggested in [8] and then further examined in [19]. Although the approach is simple, results prove to

be complicated from a signal processing perspective. There are two issues with multichannel approach in PR systems; side-lobes in both range and Doppler axis.

3.4.1 Doppler Ambiguity

The Doppler side-lobes are induced to the output of the ambiguity function is due to the different carrier frequencies of each FM channel. The Doppler shift of a target is dependent on the carrier frequency of the radar signal [6] and since each FM channel has different carrier frequencies, a single target will have different different Doppler shifts. This will induce several side-lobes in the Doppler axis at the output of the ambiguity function.

These Doppler side-lobes can be eliminated with different approaches. One of the approach is to engineer number of broadcast channels and the integration time such that, all Doppler side-lobes will fall in to the same Doppler bin, hence eliminating the side-lobes. The Doppler shift of a target is inversely proportional with the wavelength of the signal.

The Doppler shift of a target is calculated as follows:

$$f_p = \mp \frac{2v_p}{\lambda} Hz, \quad (3.2)$$

where λ is the wavelength of the signal and v_p is the radial speed of the p^{th} target. Let Δf_c is the carrier frequency difference between two consecutive broadcast channel, the following equation can be written to find the Doppler shift difference of a target for two consecutive broadcast channels:

$$\Delta f_{p_c} = \mp \frac{2v_p}{\lambda} \times \Delta f_c Hz. \quad (3.3)$$

In addition to this, Doppler resolution of a radar is inversely proportional with the integration time:

$$\Delta F_d = \frac{1}{T_i} Hz, \quad (3.4)$$

where T_i is the integration time. Thus, if the integration time is chosen such that:

$$\Delta F_d \geq m\Delta f_c, \quad (3.5)$$

where m is the number of consecutive broadcast channels to be used, the Doppler side-lobes will occur in the same Doppler, in other words, will be eliminated.

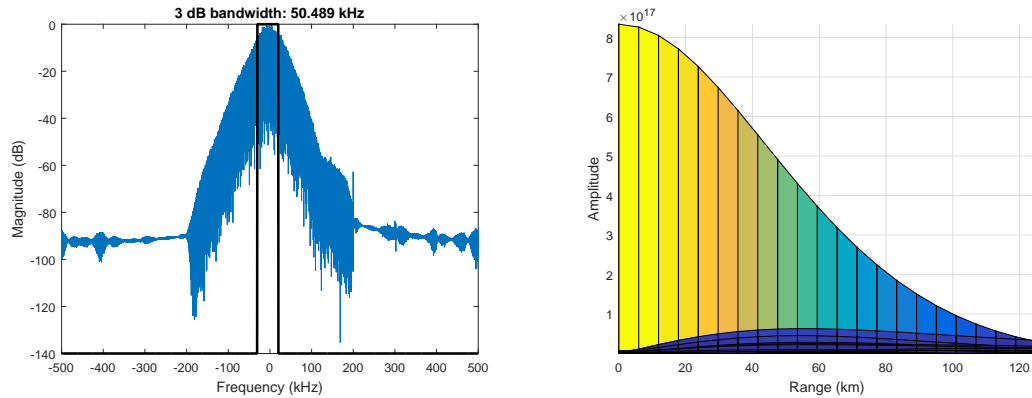
However, this method limits the system in the Doppler resolution department, in [15] Doppler side-lobes are handled in an efficient manner to overcome this limitation. Since the work in this thesis is focused on the range resolution and side-lobes in the range axis due to multichannel signals, Doppler ambiguity issue is neglected.

3.4.2 Range Ambiguity

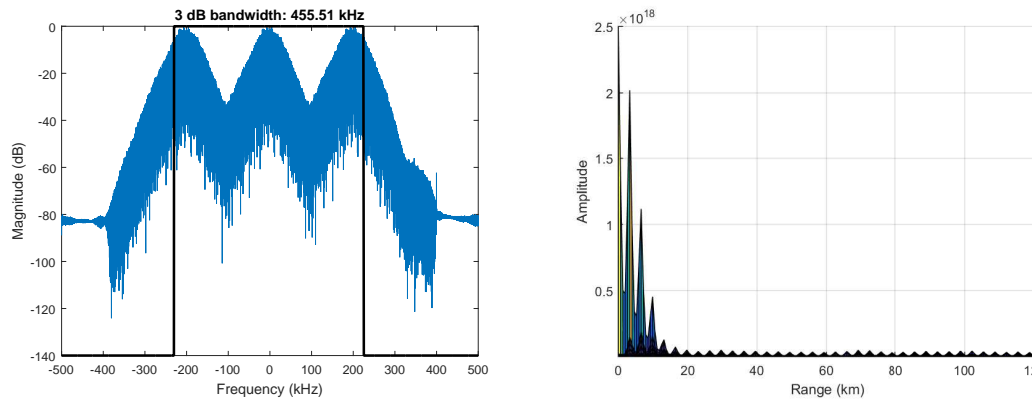
Auto-ambiguity range axis results of single channel FM and multichannel FM approach in a PR system is shown in Fig. 3.2.

From Fig. 3.2b and 3.2d, it is shown that using several consecutive channels in the PR system increases the overall bandwidth, thus better range resolution. In addition to the range resolution improvement due to the higher bandwidth, the main lobe of the output of the auto-ambiguity function is also sharp. However, this multichannel approach induces side-lobes in the range axis. This can be harmful for detection purposes when several targets are in close proximity since side-lobes might be considered as targets by the detection algorithms such as CFAR. The mathematical background of the side-lobe issue is explained in Appendix A.

In [8] a frequency domain approach is proposed to eliminate side-lobes in range axis. Frequency domain operation is somewhat able to suppress the side-lobes, but not completely. Since the approach is based on division of signals in frequency domain, such operations may induce division by 0 problems. In order to overcome division by 0, ad-hoc filtering of the signals is proposed in the approach. In [19, 15]



(a) Spectrum of a signal with single FM channel. (b) Auto-ambiguity function results of the signal in 3.2a.



(c) Spectrum of a signal with 3 FM channels. (d) Auto-ambiguity function results of the signal in 3.2c.

Figure 3.2: Comparison of single channel FM signal and 3 channel FM signal for radar purposes.

side-lobes in range axis is not addressed at all.

As a result, multichannel signals in PR systems is a viable solution to the range resolution problem, but the side-lobe issue at the output of the ambiguity function makes it imperfect. In the next chapter, not only a solution to the range resolution of single channel PR system is proposed, but also the side-lobe issue in multichannel signals in PR systems is addressed as well.

Chapter 4

Range Resolution Improvement and Elimination of Side-lobes using Deconvolution

In this chapter, we re-write the ambiguity function such that, it is a convolution of a channel impulse response with a “blurring” signal. It turns out that this “blurring” signal is actually the autocorrelation function of the transmitted signal. Thus, we show that the channel impulse response can be obtained using the autocorrelation function of the transmitted signal via deconvolution.

4.1 Ambiguity Function as a Convolution

Let $s_{ref}[n]$ be the sampled version of $s_{ref}(t)$ and $s_{surv}[n]$ be the sampled version of $s_{surv}(t)$, respectively. In this case, Eq. 2.1 becomes, be as follows, respectively.

$$s_{ref}[n] = s[n - \zeta_r], \quad (4.1a)$$

and Eq. 2.2 becomes,

$$s_{surv}[n] = \sum_{p=1}^P a_p s[n - \zeta_p] e^{j2\pi k_p n/N} + \mu[n], \quad (4.1b)$$

where $s[n]$ is the sampled version of transmitted signal, ζ_r is the sampled time delay of the transmitted signal, a_p is the attenuation of the signal echoing from the p^{th} target, ζ_p is the sampled time delay of the signal echoing from the p^{th} target, k_p is the sampled Doppler shift induced to the signal due to the speed from the p^{th} target and $\mu[n]$ is the additive noise, which is usually assumed to be i.i.d. Gaussian noise (AWGN).

Then the discrete ambiguity function $E[\zeta, k]$ is given as follows:

$$E[\zeta, k] = \sum_{n=0}^{N-1} s_{surv}[n] s_{ref}^*[n - \zeta] e^{-j2\pi kn/N}, \quad (4.2)$$

where ζ is the range bin representing the sample time delay and k is the Doppler bin representing the sampled Doppler shift. Since we want to improve the range resolution, the two dimensional matched filter in Eq. 4.2 is processed row-by-row for each Doppler shift index. Substituting Eq. 4.1a and 4.1b into Eq. 4.2, we obtain:

$$E[\zeta, k] = \sum_{n=0}^{N-1} \left[\left(\sum_{p=1}^P a_p s[n - \zeta_p] e^{j2\pi k_p n/N} + \mu[n] \right) \times s^*[n - \zeta - \zeta_r] e^{-j2\pi kn/N} \right]. \quad (4.3)$$

Next, we combine the exponential terms:

$$E[\zeta, k] = \sum_{n=0}^{N-1} \left[\left(\sum_{p=1}^P e^{j2\pi(k_p - k)n/N} a_p s[n - \zeta_p] + \nu[n] \right) \times s^*[n - \zeta - \zeta_r] \right], \quad (4.4)$$

for $k = k_p$ the exponential term will be equal to 1 and we use the k_p as a subscript

in (4.4) as follows:

$$E_{k_p}[\zeta] = \sum_{n=0}^{N-1} \left[\sum_{p=1}^P a_p s[n - \zeta_p] s^*[n - \zeta - \zeta_r] + \nu[n] s^*[n - \zeta - \zeta_r] \right], \quad (4.5)$$

where we can rearrange the sum operations as follows and make a change of variable:

$$E_{k_p}[\zeta] = \sum_{p=1}^P a_p \left[\sum_{m=0}^{N-1} s[m - \zeta_p] s^*[m - \zeta - \zeta_r] + \sum_{m=0}^{N-1} \nu[m] s^*[m - \zeta - \zeta_r] \right]. \quad (4.6)$$

The inner sum of Eq. 4.6 is the correlation of transmitted signal with its time shifted form. In addition to this, additive white Gaussian noise $\nu[m]$ and transmitted signal $s[m]$ are convolved and we obtain the signal dependent noise α . Then the ambiguity function for a fixed k_p with a simple change of variable $l = \zeta + \zeta_r$, is of the following form:

$$E_{k_p}[l] = \sum_{p=1}^P a_p r[m - l] + \alpha[l], \quad (4.7)$$

where $r[m - l]$ is the autocorrelation of the transmitted signal. Autocorrelation can be rewritten as a convolution thus Eq. 4.7 can be simplified as follows:

$$E_{k_p}[l] = (h * r)[l] + \alpha[l], \quad (4.8)$$

where $h[l]$ is the convolution of $\nu[n]$ and $s[n]$. Then the $h[l]$, the channel impulse response, is defined as follows:

$$h[l] = \sum_{p=1}^P a_p \delta[l - \zeta_p]. \quad (4.9)$$

It is a time-invariant system representing the delays of target echoes. Eq. 4.8 is equivalent to 4.2, thus deconvolution can be used for reversing the convolution operation in 4.8. After solving the ordinary matched filter and obtaining the range-Doppler map, the deconvolution approach is used as a post processing method for further analysis. Since in a PR system, $s_{ref}[n]$ is already needed to solve the matched filter, thus $r[l]$ can be computed and is available. A PR system also computes $E_k[l]$, therefore channel impulse response $h[l]$ can be estimated using complex deconvolution. An example iterative complex deconvolution algorithm is applied as follows [20, 21]:

$$h_{i+1} = \lambda E_{k_p} + \left(h_i - \lambda(r * h_i) \right), \quad (4.10)$$

where h_i is the current iterate of the complex channel impulse response, E_{k_p} is the p^{th} line of the complex range-Doppler map output, λ is a regularization parameter and $*$ is the convolution operation. In addition to this, it is experimentally observed that, applying the deconvolution scheme on to the magnitude of the complex signals is possible and presented in the experimental analysis section.

When $k \neq k_p$ ambiguity function takes significantly low values compared to $k = k_p, p = 1, 2, \dots, P$ case and the deconvolution process will not effect the output of the ambiguity function.

This approach improves the performance of the multichannel FM based PBR systems as well. In the multichannel FM signal case, deconvolution approach reduces side-lobes significantly and results in cleaner outputs. This is due to the deconvolution approach being based on to the correlation of signals. Since the multichannel signal end up with side-lobes at the output of the correlation function, both $r[l]$ and $E[\zeta, k]$ will have the same side-lobes, thus Eq. 4.8 can be applied to the multichannel signals without additional problem.

In other words, autocorrelation of the transmitted signal is “blurred” by a point spread function (PSF). In non-blind deconvolution algorithms, it is assumed that this PSF is known. With this point of view, it is possible to approach the ambiguity function from both one dimensional (1-D) and two dimensional (2-D)

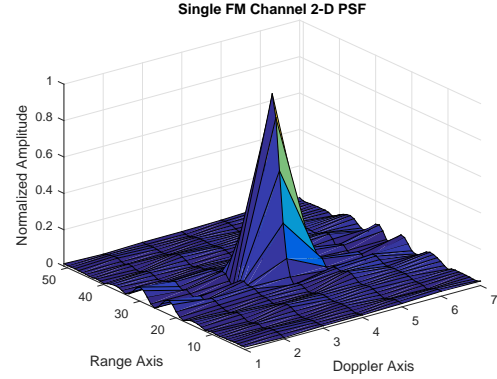
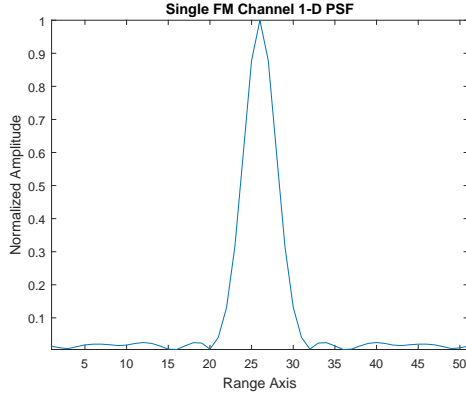
perspective.

In the 1-D approach, the PSF is a 1-D signal, the autocorrelation of the transmit signal. The ambiguity function is then deconvolved row-by-row for each Doppler bin. Row-by-row computation enables high parallelism for faster computation and in most cases, it is not necessary to solve the whole range-Doppler map. Since range-Doppler map is already computed, it is enough to submit only rows with peaks to deconvolution, which further decreases the computational load. In the 2-D approach, PSF is the auto-ambiguity of the transmit signal. 2-D deconvolution does not support the high parallelism 1-D enables, but there are efficient 2-D deconvolution algorithms. Typical 1-D and 2-D PSFs for deconvolution of ambiguity function is shown in Fig. 4.1. Using either 1-D or 2-D PSFs, it is possible to deconvolve the output of the ambiguity function and estimate the channel impulse response. In this thesis, four different deconvolution methods are used, two 1-D and two 2-D. 1-D methods are Iterative Complex Deconvolution in Eq. 4.10 and Fourier-Wavelet Regularized Deconvolution (ForWaRD-WaRD1D) [22]. 2-D methods are, Lucy-Richardson Deconvolution Algorithm [23] and an extension to the DAMAS algorithm called DAMAS3 [24]. Since DAMAS3 algorithm is the best performing deconvolution algorithm, it is briefly explained in Appendix B.

The same conclusion can be reached using Fourier domain approach in [8]. The approach can be summarized as follows in continuous time domain taking Eq. 2.2 and 2.1 in to the consideration. The cross correlation of 2.2 with 2.1 at delay τ is given by:

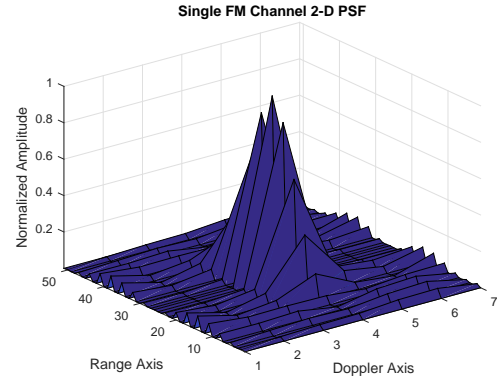
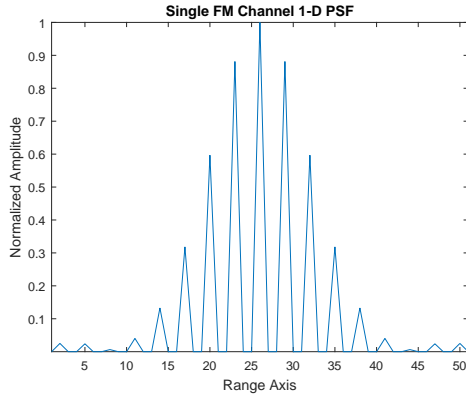
$$c(\tau) = \sum_{p=1}^P a_p r(\tau - t_p) + n(\tau) * s(\tau), \quad (4.11)$$

where a_p is the attenuation of the signal echoing from obstacle p , t_p is the time delay of the signal echoing from obstacle p , $r(\cdot)$ is the autocorrelation of the direct signal and $n(\tau) * s(\tau)$ is the convolution of noise and the direct signal.



(a) 1-D PSF for solving deconvolution of range-Doppler map of a PR system using single FM channel.

(b) 2-D PSF for solving deconvolution of range-Doppler map of a PR system using single FM channel.



(c) 1-D PSF for solving deconvolution of range-Doppler map of a PR system using three FM channels.

(d) 2-D PSF for solving deconvolution of range-Doppler map of a PR system using three FM channels.

Figure 4.1: Several PSF examples used to solve deconvolution problem in FM based PR systems.

Next, Fourier transform of Eq. 4.11 is obtained:

$$C(f) = \sum_{p=1}^P a_p e^{-j2\pi f t_p} F\{r(\tau)\} + \sqrt{N_0} S(f), \quad (4.12)$$

where $F\{r(\tau)\}$ is the continuous time Fourier transform of the autocorrelation function, $N_0 = kT_0 B$ is the power spectral density of the white noise and $S(f)$ is the Fourier transform of the direct signal [8]. In [8], the Eq. 4.12 is divided by

$|S(f)|^2$ and the following equation is obtained:

$$\frac{C(f)}{|S(f)|^2} = \sum_{p=1}^P a_p e^{-j2\pi f t_p} + \frac{\sqrt{N_0}}{S(f)}. \quad (4.13)$$

Eq. 4.13 basically corresponds to the frequency domain deconvolution operation. However, division by $|S(f)|^2$ may not be possible for $|S(f)|^2 \approx 0$. To prevent this problem the division operation is performed only at low frequencies in [8]. Time domain deconvolution eliminates division by zero problem.

Eq. 4.12 can be also expressed as follows:

$$C(f) = |S(f)|^2 \sum_{p=1}^P a_p e^{-j2\pi f t_p} + \sqrt{N_0} S(f). \quad (4.14)$$

The inverse Fourier transform of both sides lead to:

$$c(\tau) = r(\tau) * h(\tau) + n(\tau) * s(\tau), \quad (4.15)$$

where $h(\tau) = F^{-1}\{\sum_{p=1}^P a_p e^{-j2\pi f t_p}\}$ which is the channel impulse response. Eq. 4.8 is the discrete time version of Eq. 4.13.

4.2 Experiment Setup and Results of Deconvolution Algorithms

In this chapter, we describe the experimental setup for both single and multi channel FM based PR system, application of deconvolution algorithm to estimate the channel impulse response and results of said algorithms. Unfortunately, due to the lack of real data, we created the FM signals and the radar scenario with targets and clutters in computer environment. In this chapter, generation of FM signals, the receiver structure and the steps of deconvolution algorithm is further explained. A performance measure for deconvolution algorithms for the purpose of range resolution improvement in PR systems is proposed. Several experimental

results are shown.

4.2.1 FM Radio Signals for Passive Radar in Computer Environment

In order to generate FM radio signals in the computer environment for the purpose of passive radars, we first developed a similar template as in [11]. We also take the FM radio standards in to consideration in [10] and created a template in Matlab for generation of complex baseband FM radio signal. The block diagram of the template is in Fig. 4.2.

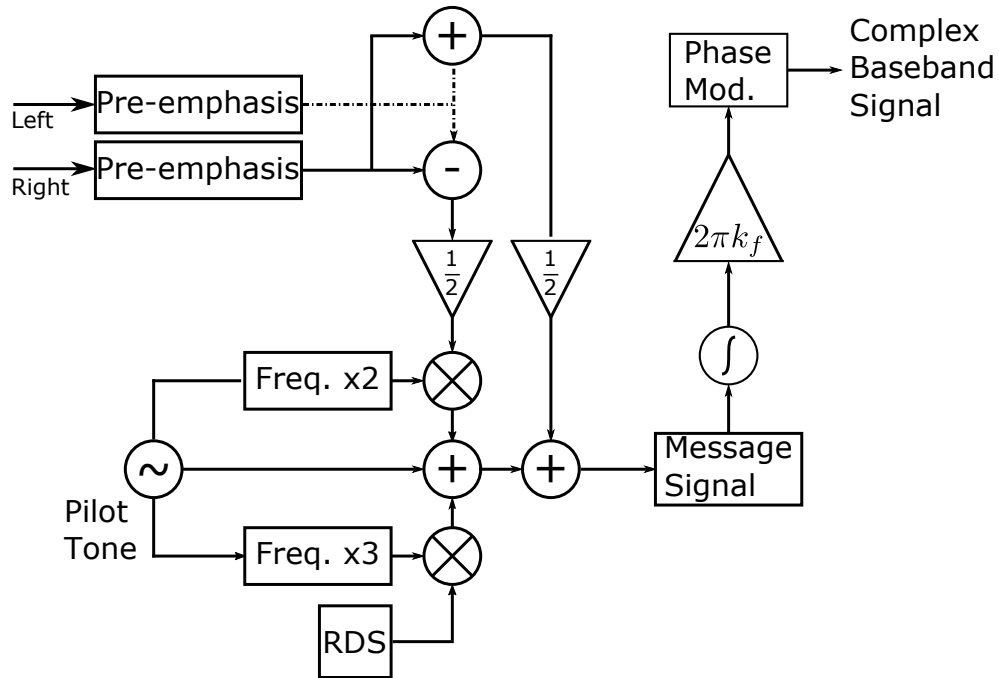


Figure 4.2: Template for stereophonic complex baseband FM signal generation.

In Fig. 4.2, *Left* and *Right* are the left and right channel data respectively. Pilot tone is set as 19 kHz in the FM radio standards [10]. RDS is the radio data system that is used to carry auxiliary data, e.g. weather forecast, genre of the song or traffic information. Message signal is also called the radiophonic signal. k_f is the maximum frequency deviation and is set as 75 kHz in the FM radio

standards [10].

The block diagram in Fig. 4.2 can be extended to create multichannel FM signals as well. Generally, several FM channels are being broadcast from a single antenna site and it is possible to gather a number of FM channels using a receiver with high bandwidth. As mentioned before, this practically increases the range resolution however, also induces a side-lobe issue which we aim to solve with deconvolution methods. In order to simulate multichannel FM signals in a computer, we first need to create several complex baseband FM signals with the block diagram given in Fig. 4.2. Then we combine these complex baseband FM signals with the following fashion shown in Fig. 4.3.

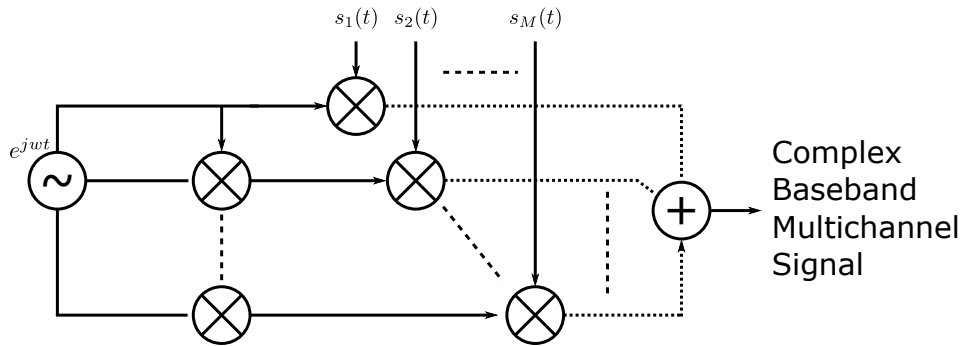


Figure 4.3: Template for complex baseband multichannel FM signal generation.

In Fig. 4.3, $\omega = 2\pi\Delta Ft$ where ΔF corresponds to the frequency distance between the midpoints of two FM channels, $s_1(t), s_2(t), \dots, s_M(t)$ are M different FM channels. M FM channels are in fact concatenated in the frequency domain with midpoint distance ΔF . Thus, we are able to create a multichannel FM signal in the baseband. An example multichannel FM signal with three channels is shown in Fig. 3.1c.

In reality, a multichannel FM signal can only be gathered using a receiver with high bandwidth. After the reception of signal, it is possible to divide the signal into different FM channels and then rebuild a new multichannel FM signal using the same block diagram in Fig. 4.3 as well. This approach enables system to create multichannel FM signals with different distances between channels in frequency domain. The effect of rearrangement of the FM channels in the frequency domain

is further investigated in the upcoming sections.

The environment scenario is then generated with the following block diagram in Fig. 4.4.

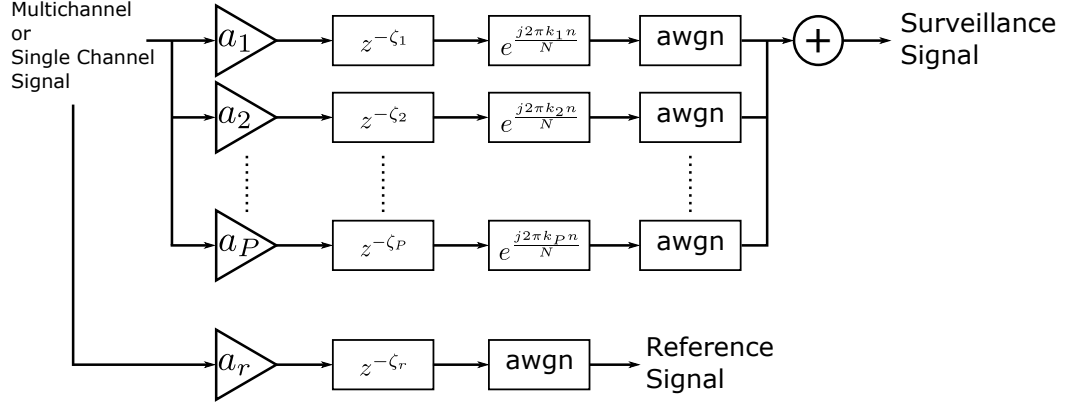


Figure 4.4: Template for scenario generation.

In Fig. 4.4, it is assumed that there are P objects in the detection range of the radar. a_1, a_2, \dots, a_P corresponds to the complex attenuation of the complex baseband FM signal echoing from 1, 2, \dots , P objects. $\zeta_1, \zeta_2, \dots, \zeta_P$ corresponds to the sample delay of P objects caused by their distances. k_1, k_2, \dots, k_P corresponds to the Doppler shift of the each object's relative speed. For stationary objects such as hills or buildings, Doppler shift is taken as zero. *awgn* corresponds to the channel's additive white Gaussian noise. a_r is the complex attenuation of the reference signal. ζ_r is the time delay of the reference signal that is caused by the distance between transmitter and receiver antenna. The reference signal does not have any Doppler shift unless the receiver antenna is moving. In this thesis, it is assumed that the receiver antenna is stationary.

Block diagrams in Fig. 4.2, 4.3 and 4.4 are used in this thesis to generate the corresponding FM based PR signals.

4.2.2 Passive Radar Receiver with Deconvolution Post Processing

In reality, it is expected that there are stationary objects, also called clutters, in the detection range of a PR system. Most of the time, these clutters create unwanted, powerful peaks at the output of the matched filter which prevent detection of actual targets of interest. Thus, it is important that we clear the surveillance signal from these clutter echoes. The conventional method of clearing the clutter echoes from the surveillance signal is to use adaptive filters.

Fig. 4.5 is the block diagram of the PR system of concern. The reference and surveillance signals are gathered from different antennas. If the signals are single channel, they are directly fed to the adaptive filter and the error of the adaptive filter is the surveillance signal with clutters suppressed about 30 dB. If the signals are multichannel, then each channel have to be down converted to baseband and filtered out with a low pass filter (LPF) so that they are turned into several single channel FM signals. These channels are fed to different adaptive filters in parallel and then assembled again to generate the multichannel signal, without affects of clutter this time.

After the clutter removal, the error signal and the reference signal are fed to the matched filter block in order to generate the 2-D range-Doppler map. In addition to this, the reference signal fed to “matched filter for PSF” block to generate the corresponding PSF, with itself. Then the deconvolution algorithm of concern is run at the deconvolution block with the range-Doppler map and the PSF as inputs. The output of the deconvolution algorithm is expected to generate impulse-like shapes at the range and Doppler of actual targets with increased performance on target separation in the case of single channel FM signals and decrease at the overall side-lobe power in the case of multichannel FM signals.

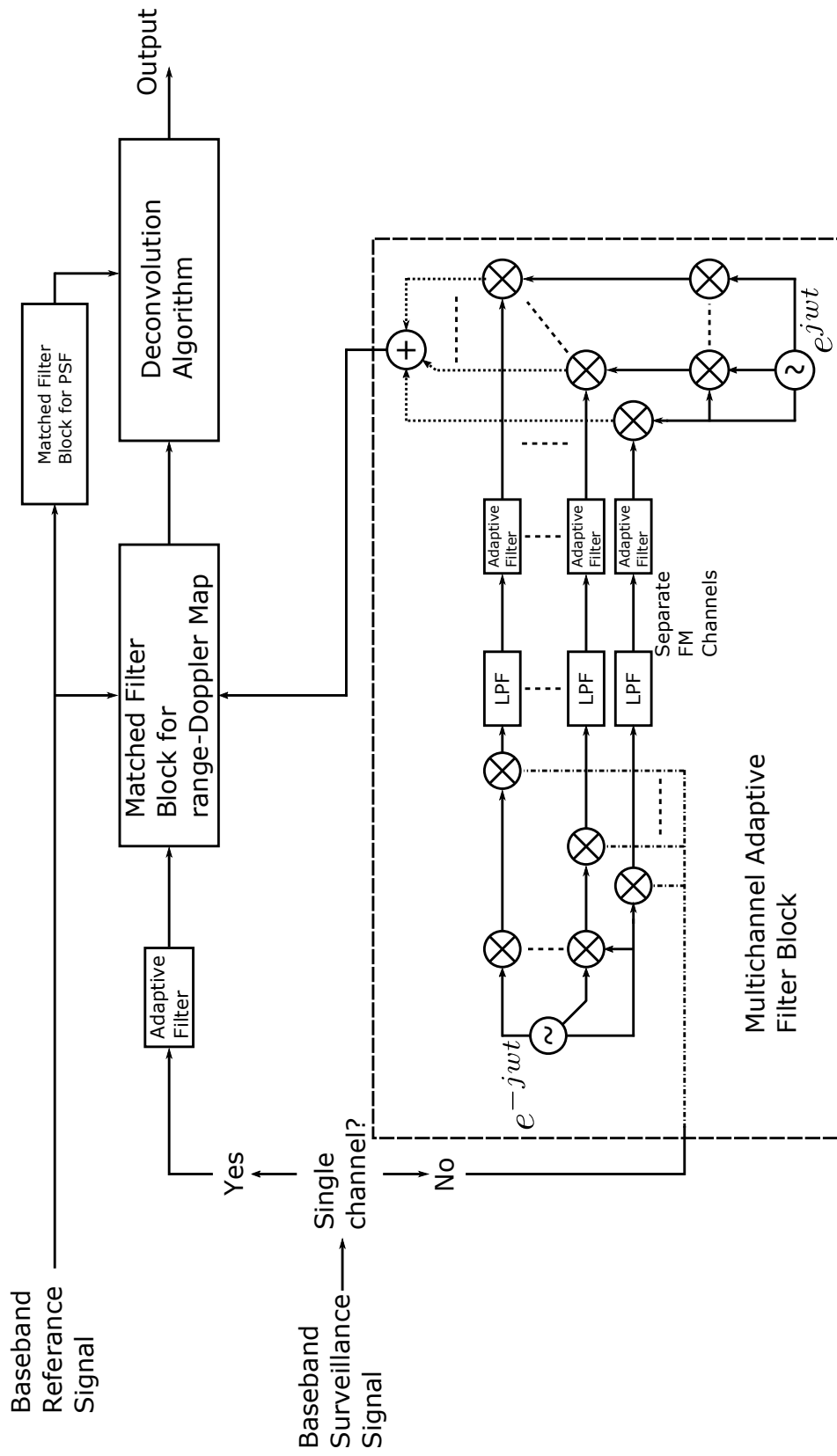


Figure 4.5: Template for receiver block.

4.2.3 Performance Measures

Performance measure for single channel FM signal case is the successful separation of the targets. In a typical radar, two targets are assumed to be two distinct targets, if there is a 3 dB dip between them [6]. This is called in this thesis as “3-dB separation performance”. An example of two targets that are not separated in the 3-dB separation sense is shown in Fig. 4.6. Since the dip between targets is below 3 dB, targets are considered as not separated.

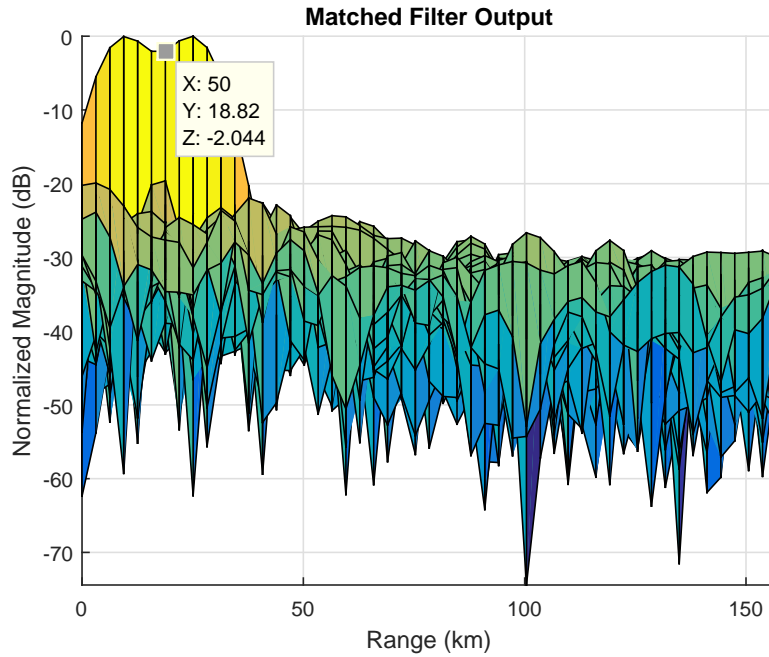
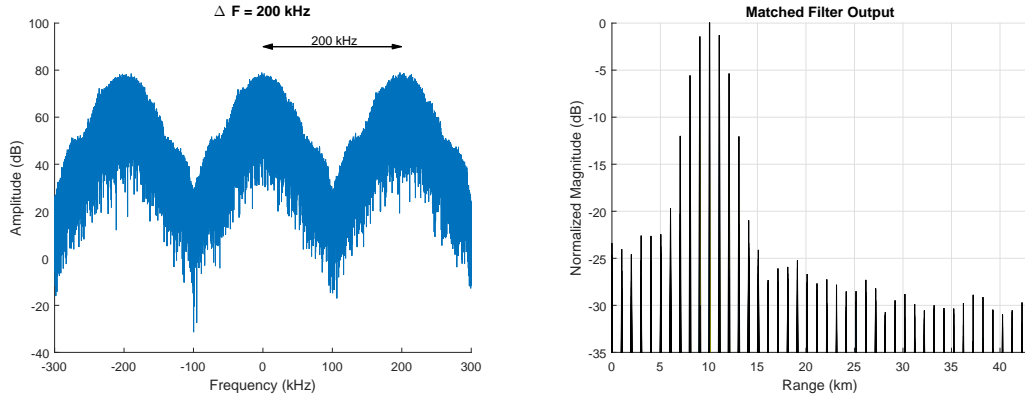


Figure 4.6: 3-dB separation example with two targets at 10 and 26 km.

One of the performance measures for multichannel FM signals is the suppression of side lobes due to the frequency distance between two FM channels, namely ΔF . The mathematical reasons for the side lobes in multichannel FM signals at the output of the matched filter is explained in Appendix A. It is shown that the output of the matched filter is modulated with the ΔF , thus decreasing ΔF will also decrease the side lobe amplitudes, with a range resolution trade off. An example of effect of different ΔF on the output of the matched filter is shown in Fig. 4.7. When the ΔF is small, the side lobes are significantly below the actual target peaks, however as a trade off, the bandwidth is narrower thus the range

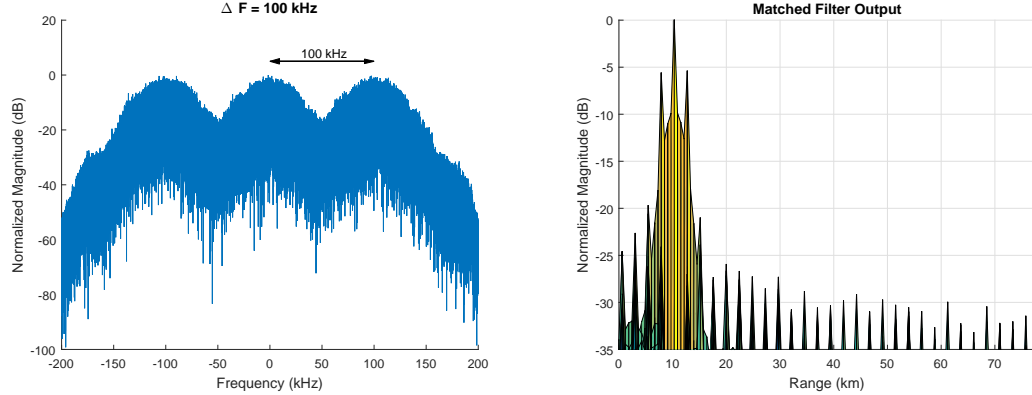
resolution is lesser compared to the $\Delta F = 200$ kHz case.

In reality, two FM channels are separated by about $\Delta F = 200$ kHz. It is possible to decrease this ΔF with simple signal processing blocks and achieve a so called “signals with nested FM channels”.



(a) A multichannel signal with 3 FM channels and $\Delta F = 200$ kHz.

(b) Matched filter output of Fig. 4.7a with one target at 10 km.



(c) A multichannel signal with 3 FM channels and $\Delta F = 100$ kHz.

(d) Matched filter output of Fig. 4.7c with one target at 10 km.

Figure 4.7: Several PSF examples used to solve deconvolution problem in FM based PR systems.

Final performance measure for multichannel FM signal case is the suppression of side lobes that occur at the output of the matched filter due to the deconvolution method. These side lobes tend to be as powerful as 1.2 dB below the main peak that belongs to the target and when there are several targets in close proximity of each other, side lobes tend to overlap and further enhance each other. In the deconvolution method, the performance measure is, how much these side

lobes are suppressed in dB. Nested FM channels also affect the output of the deconvolution post processing and is further investigated in the Experimental Results chapter.

4.2.4 Simulation Results

In the first simulation set, the separation of targets in single FM channel case is investigated. For this purpose, a scenario in which two targets are approaching to each other in time and several clutters are created. The scenario is shown in Table 4.1.

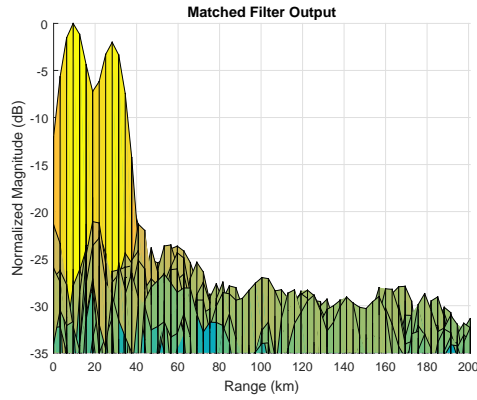
Table 4.1: Scenario for the first experiment on separation of targets.

	Bistatic Distance to Receiver (Km)	Doppler Shift (Hz)	SNR (dB)
Target ₁	10	20	-3
Target ₂	27	20	-5
Clutter ₁	2	0	10
Clutter ₂	4	0	7
Clutter ₃	5	0	8
Clutter ₄	12	0	5

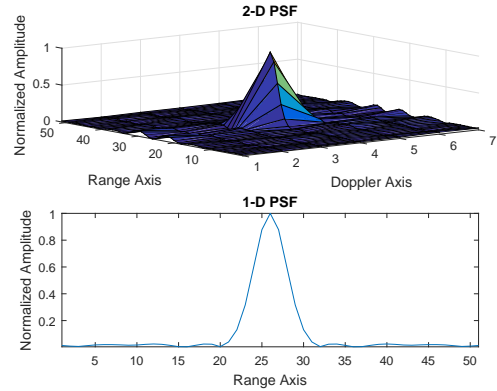
When the reference and surveillance signals are gathered by the radar, they are at first sent to the adaptive filter block for clutter removal. Then the output of the adaptive filter and reference signal are fed to the matched filter block and the deconvolution algorithms of concern are run over this output. The results are in Fig. 4.8.

As it is shown in Fig. 4.8a, matched filter is barely able to separate the targets in the 3-dB sense, where as all the deconvolution algorithms can easily separate the target. In Fig. 4.9, performance of the deconvolution approach when the distance between targets are 10 km is shown. The first target is at 10 km with SNR -3 dB and second target at 20 km with SNR -5 dB.

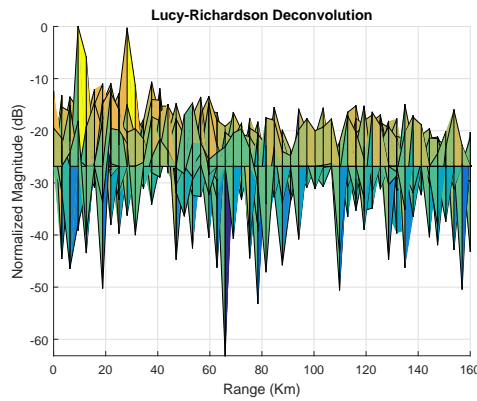
In Fig. 4.9, it is shown that when the targets have about 10 km distance



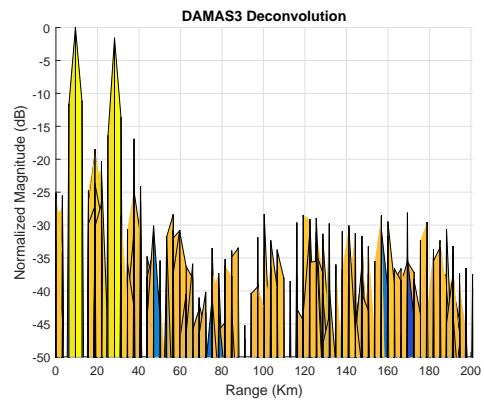
(a) Matched filter output of the scenario in Table. 4.1.



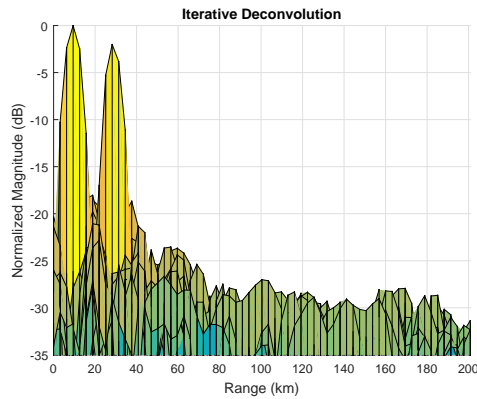
(b) 2-D and 1-D PSFs.



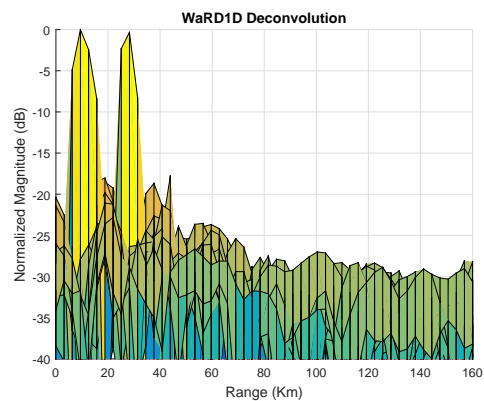
(c) Output of 2-D Lucy-Richardson deconvolution algorithm.



(d) Output 2-D DAMAS3 algorithm.

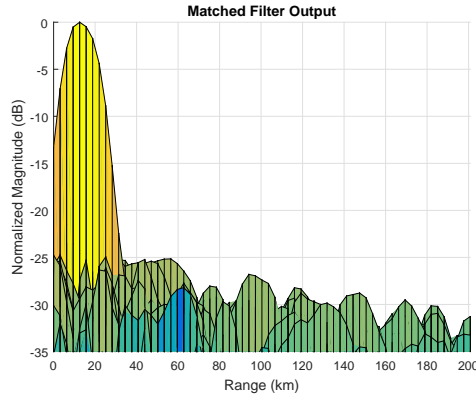


(e) Output of 1-D Complex Iterative Deconvolution.

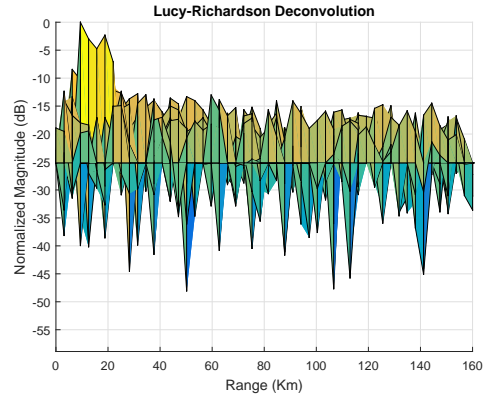


(f) Output of 1-D WaRD1D algorithm.

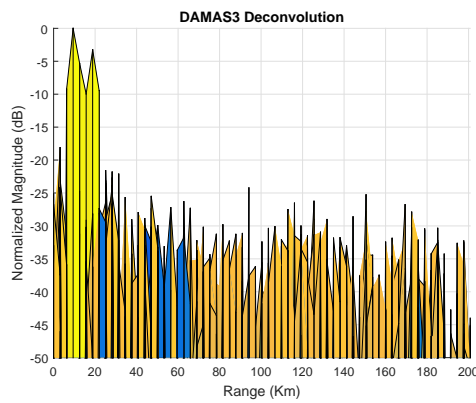
Figure 4.8: Results of the first experiment in Table 4.1.



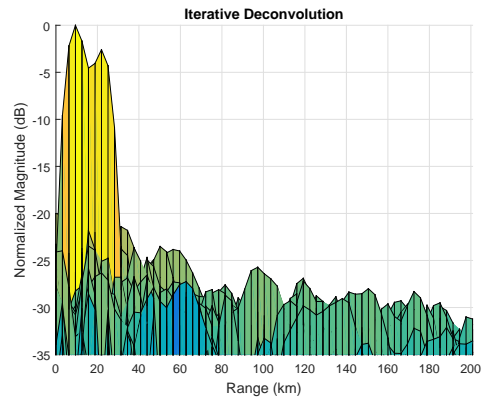
(a) Matched filter output of the second case, targets are at 10 and 20 km.



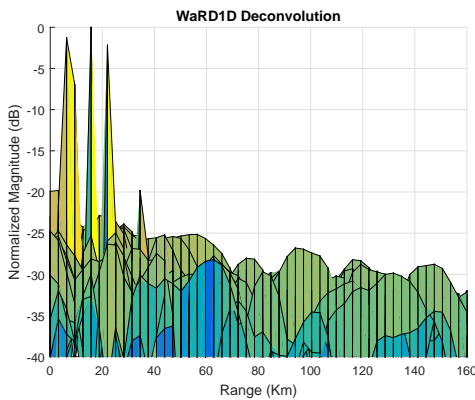
(b) Output of 2-D Lucy-Richardson deconvolution algorithm.



(c) Output 2-D DAMAS3 algorithm.



(d) Output of 1-D Complex Iterative Deconvolution.



(e) Output of 1-D WaRD1D algorithm.

Figure 4.9: Results of the first experiment with first target at 10 km and second target at 20 km.

between them, matched filter fails to separate the targets as distinct peaks. However, Lucy-Richardson algorithm, DAMAS3 and Iterative Complex Deconvolution methods are still able to separate the targets in the 3-dB separation sense. WarD1D algorithm fails to resolve targets. Thus we can conclude that the 10 km distance between the targets is a threshold for the performance of these three deconvolution algorithms, and that the deconvolution method effectively increases the target separation in a FM based PR system. In the light of these experiments, the comparison graph in Fig. 4.10 is obtained. It is clear that all deconvolution algorithms increased the range resolution performance of a single channel FM signal based PR system compared to the matched filter.

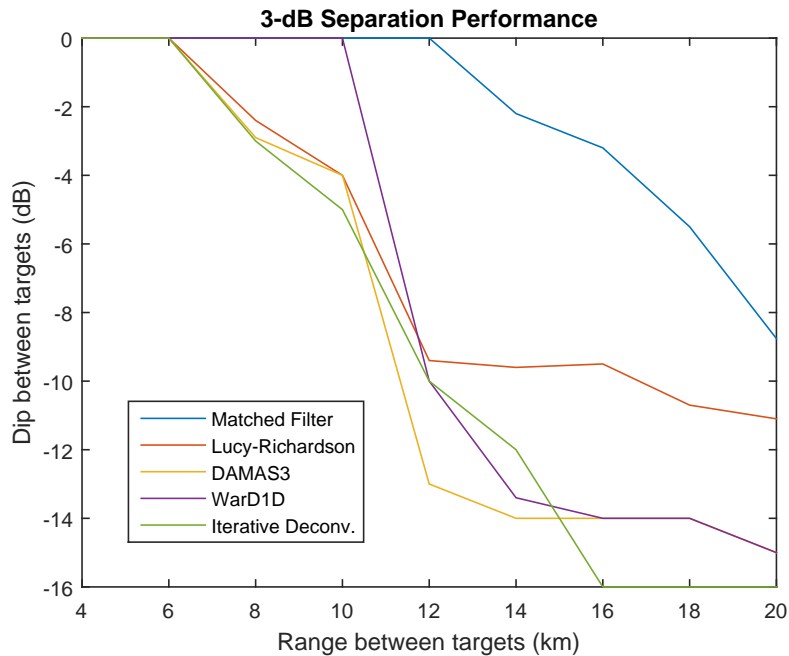


Figure 4.10: Comparison of 3-dB separation performance of matched filter and deconvolution algorithms with respect to range.

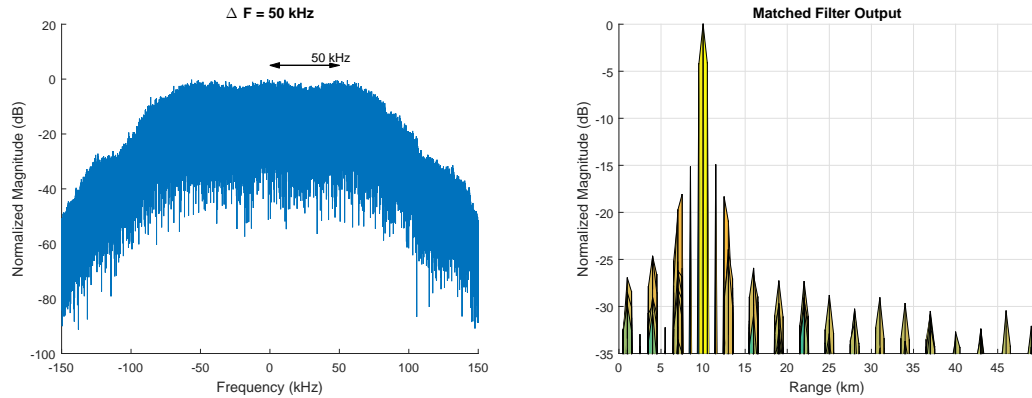
The multichannel FM signal method is proposed as a solution to the low range resolution in FM based PR systems. Since a signal with multiple consecutive FM channels provide a wider bandwidth signal, range resolution can be increased without a problem. However, the multichannel FM signal comes with a side lobe issue which harms the successful detection of actual target peak. In Fig. 4.7b, a single target at 10 km, 10 Hz is induced on to a multichannel FM signal with

three FM channels and the target is found with matched filter. The highest side lobes are about 1.2 dB below the actual target peak, preventing healthy detection of actual target location. In addition to this, if there are two targets in close proximity, the side lobes add in a destructive way and start to have more amplitude compared to actual target peaks.

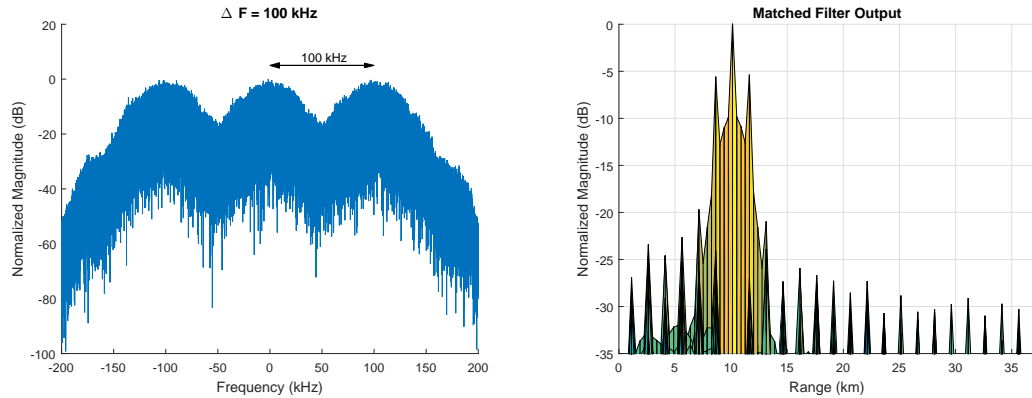
Since it is not needed to increase the range resolution in multichannel FM signal case, the aim is to decrease the side lobe amplitudes. There are two possible ways to achieve lower side lobes. First is to rearrange the signals in the frequency domain and decrease the separation between two FM channels in frequency domain by decreasing ΔF . Second is to apply deconvolution on to output of the matched filter.

Amount of ΔF affects the deconvolution performance, thus at first, effect of ΔF on the amplitude of side lobes is investigated. For this purpose, a single target at 10 km and 20 Hz Doppler shift is created on a signal with 3 FM channels. Results for 4 different ΔF values are shown in Fig. 4.11 and 4.9.

From Fig. 4.11 and 4.12, it can be seen that the ΔF has a direct effect on the side lobe magnitude. As the separation between FM channels is decreased, the side lobe magnitude also decreases significantly. However, this approach comes with a trade off in range resolution. With the “nested channel” approach, the PR system can still benefit from the wider bandwidth of the multichannel and at the same time lower the side lobe levels as well. A “ ΔF vs. Highest Side lobe level” for a signal with three FM channels is shown in Fig. 4.13.



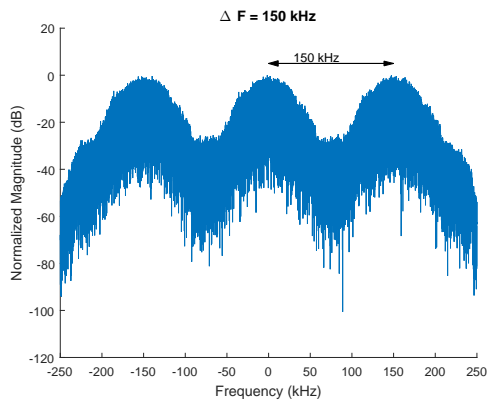
(a) A multichannel FM signal with three channels, $\Delta F = 50$ kHz. (b) Matched filter output of the signal in Fig. 4.11a with single target at 10 km.



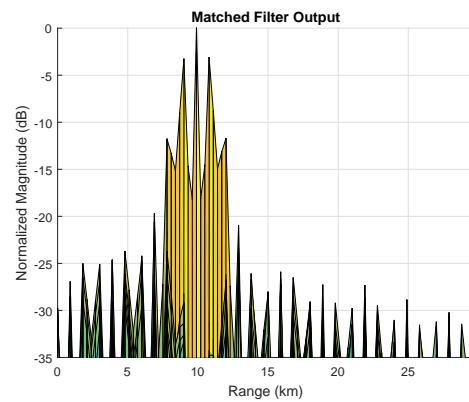
(c) A multichannel FM signal with three channels, $\Delta F = 100$ kHz. (d) Matched filter output of the signal in Fig. 4.11c with single target at 10 km.

Figure 4.11: Results of the second experiment with a single target at 10 km for $\Delta F = 50, 100$ kHz.

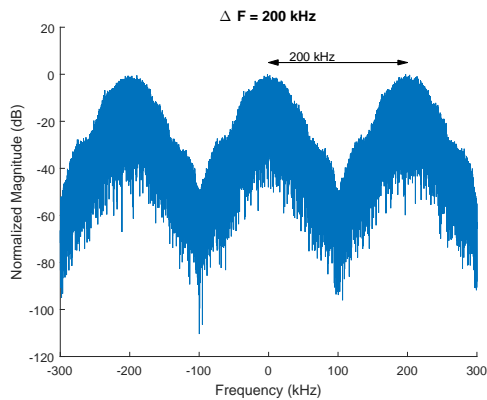
In the last experiment setup, the deconvolution algorithm is applied on to the matched filter output of a multichannel FM signal based PR system. Effect of deconvolution algorithm regarding to the side lobe levels is investigated for different ΔF values. The scenario in this experiment is in Table 4.2. In the scenario, the targets are 6 km apart from each other. This is significantly below what a single channel FM based PR system can resolve with both the standard matched filter and the deconvolution post processing. Additionally, for the multichannel FM based PR systems, since the number of channels used in the PR system can be increased, range resolution is a secondary issue compared to the side lobes that are close to the target peaks. The clutters are successfully removed from



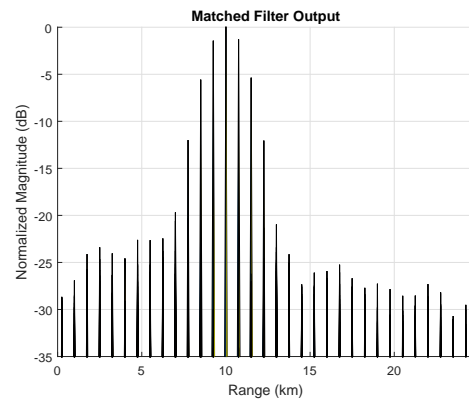
(a) A multichannel FM signal with three channels, $\Delta F = 150$ kHz.



(b) Matched filter output of the signal in Fig. 4.12a with single target at 10 km.



(c) A multichannel FM signal with three channels, $\Delta F = 200$ kHz.



(d) Matched filter output of the signal in Fig. 4.12c with single target at 10 km.

Figure 4.12: Results of the second experiment with a single target at 10 km for $\Delta F = 150, 200$ kHz.

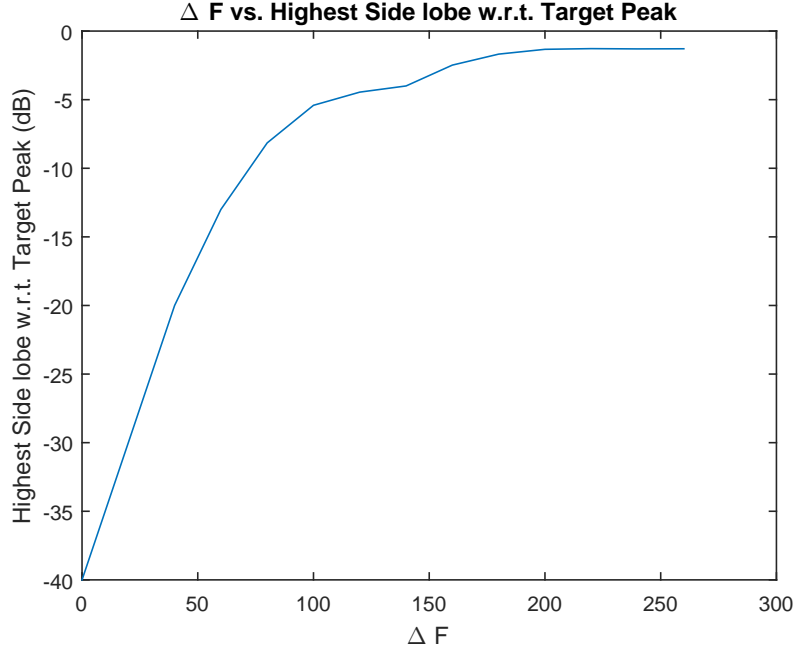


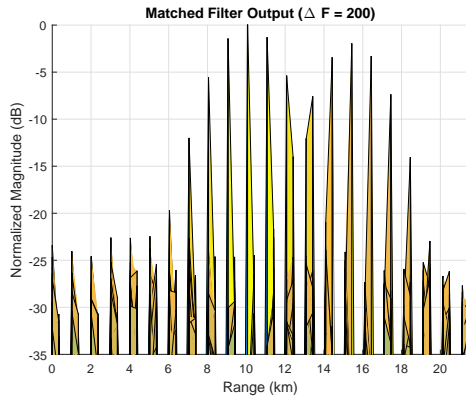
Figure 4.13: Effect of ΔF on the side lobe amplitude.

the surveillance signal using the multichannel adaptive filtering block in the Fig. 4.5. The results of this experiment is shown in Fig. 4.14, 4.15, 4.16 and 4.17.

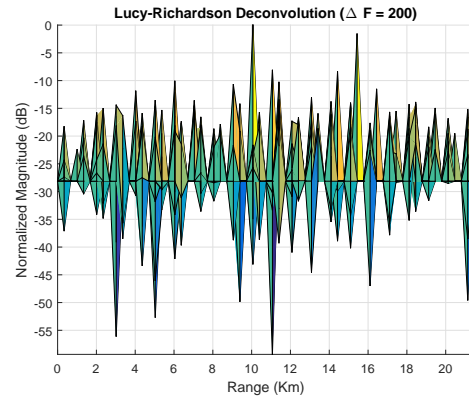
Table 4.2: Scenario for the first experiment on separation of targets.

	Bistatic Distance to Receiver (Km)	Doppler Shift (Hz)	SNR (dB)
Target ₁	10	20	-3
Target ₂	16	20	-5
Clutter ₁	2	0	10
Clutter ₂	4	0	7
Clutter ₃	5	0	8
Clutter ₄	12	0	5

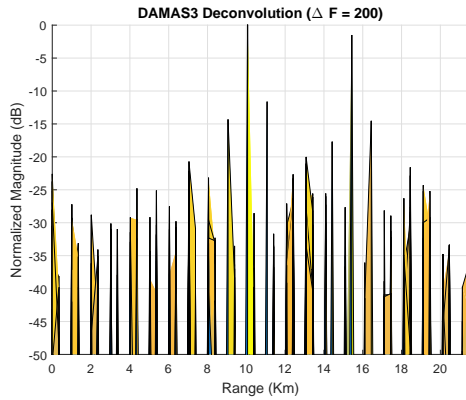
From the Fig. 4.14, 4.15, 4.16 and 4.17, the performance of the deconvolution algorithm is clear. For $\Delta F = 200$ kHz case, Lucy-Richardson and DAMAS3 algorithms managed to suppress the side lobes down to -7 and -12 dB respectively from -1.22 of the matched filter. The 1-D Iterative Complex Deconvolution also manages to achieve good results at $\Delta F = 200$ kHz. WarD1D on the other



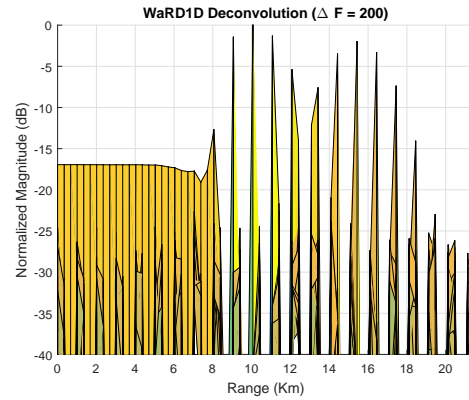
(a) Matched filter output of the scenario in Table 4.2 with $\Delta F = 200$ kHz.



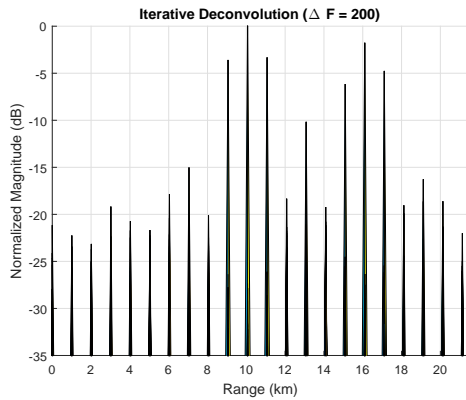
(b) Lucy-Richardson post processing of the matched filter output in Fig. 4.14a.



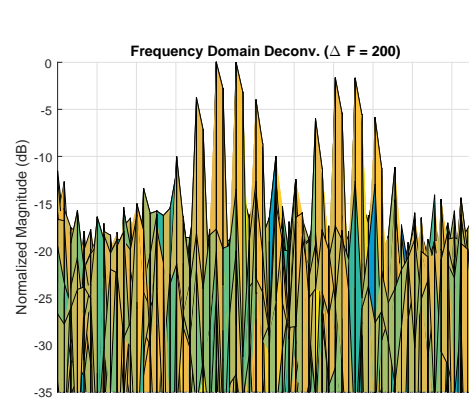
(c) DAMAS3 post processing of the matched filter output in Fig. 4.14a.



(d) WarD1D post processing of the matched filter output in Fig. 4.14a.

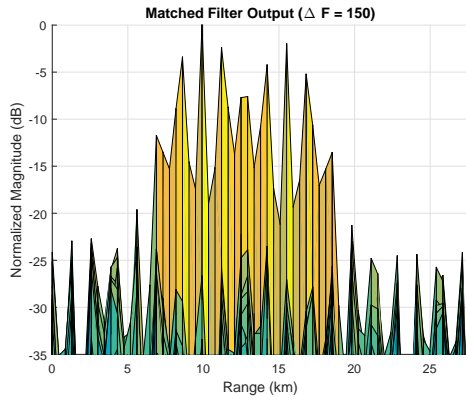


(e) Iterative Complex Deconv. post processing of the matched filter output in Fig. 4.14a.

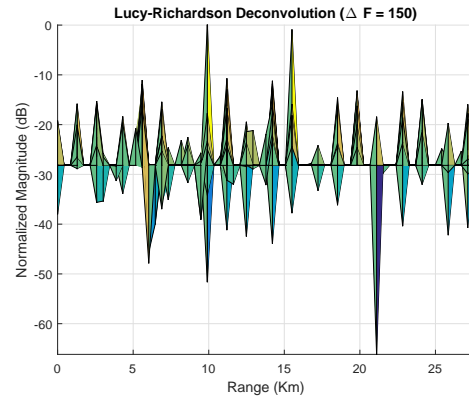


(f) Frequency domain deconvolution.

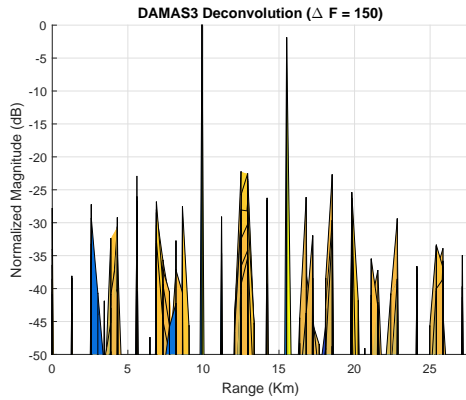
Figure 4.14: Results of the third experiment with scenario in Table 4.2 and $\Delta F = 200$ kHz.



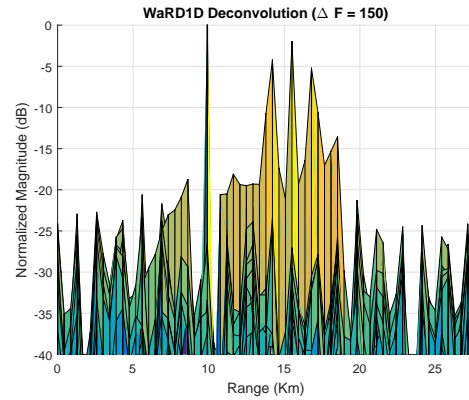
(a) Matched filter output of the scenario in Table 4.2 with $\Delta F = 150$ kHz.



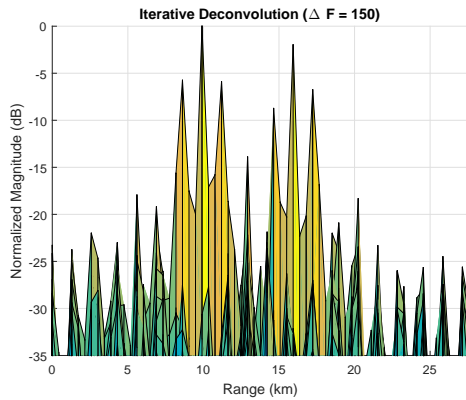
(b) Lucy-Richardson post processing of the matched filter output in Fig. 4.15a.



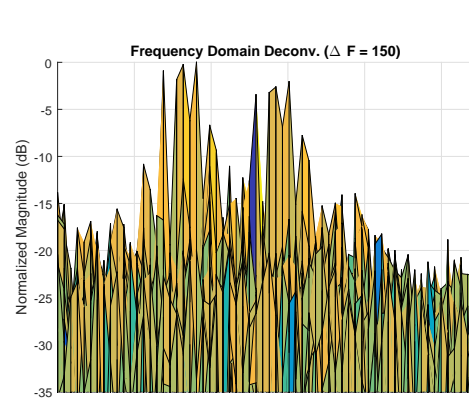
(c) DAMAS3 post processing of the matched filter output in Fig. 4.15a.



(d) WarD1D post processing of the matched filter output in Fig. 4.15a.

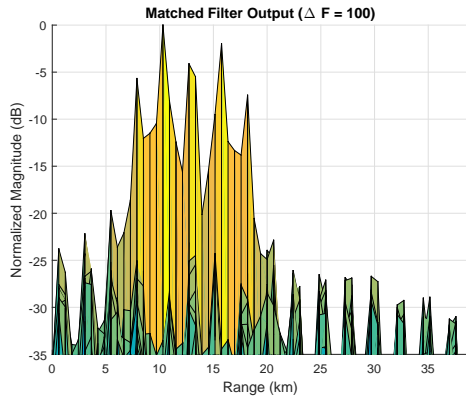


(e) Iterative Complex Deconv. post processing of the matched filter output in Fig. 4.14a.

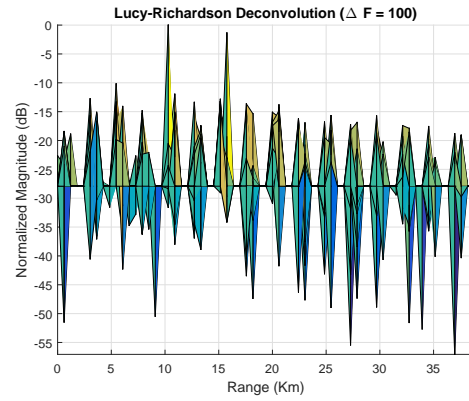


(f) Frequency domain deconvolution.

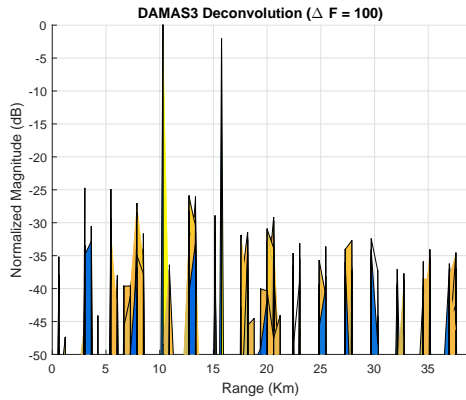
Figure 4.15: Results of the third experiment with scenario in Table 4.2 and $\Delta F = 150$ kHz.



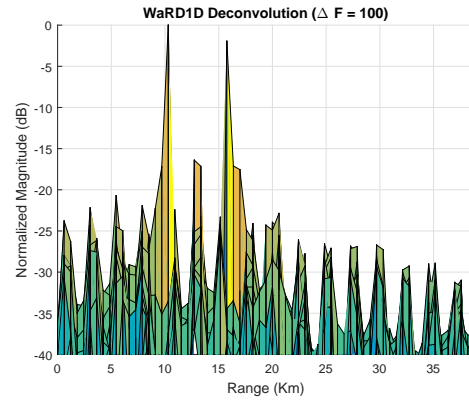
(a) Matched filter output of the scenario in Table 4.2 with $\Delta F = 100$ kHz.



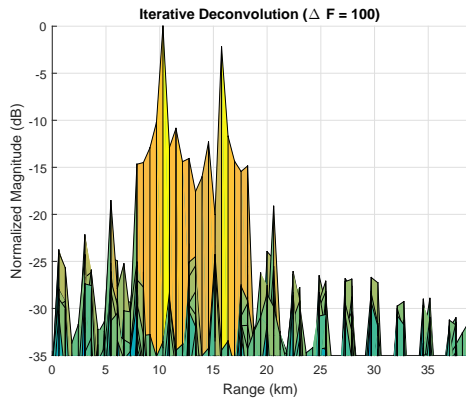
(b) Lucy-Richardson post processing of the matched filter output in Fig. 4.16a.



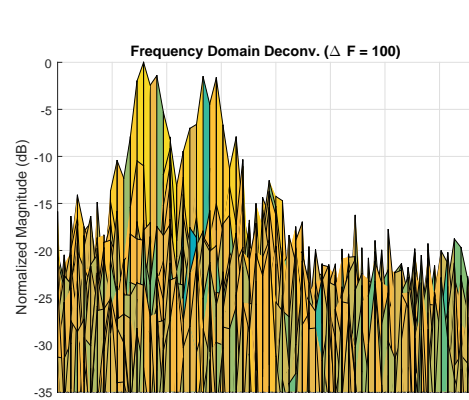
(c) DAMAS3 post processing of the matched filter output in Fig. 4.16a.



(d) WarD1D post processing of the matched filter output in Fig. 4.16a.

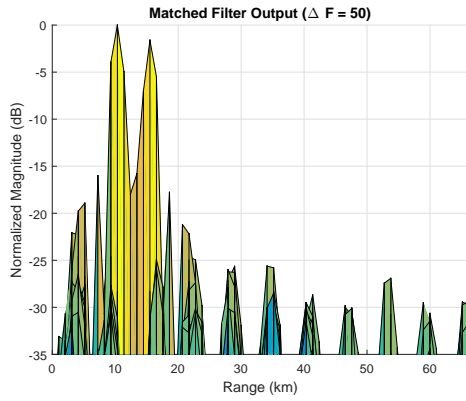


(e) Iterative Complex Deconv. post processing of the matched filter output in Fig. 4.14a.

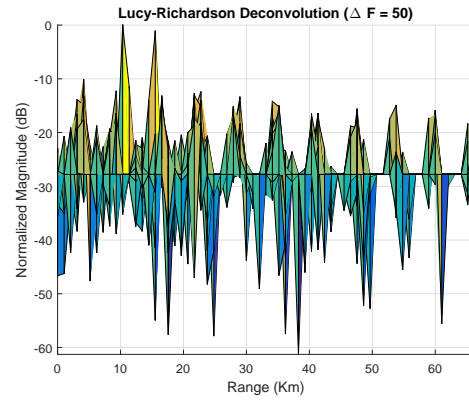


(f) Frequency domain deconvolution.

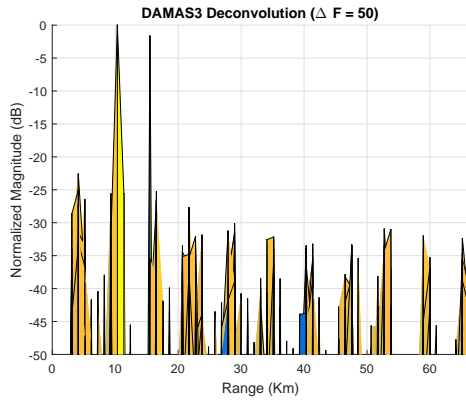
Figure 4.16: Results of the third experiment with scenario in Table 4.2 and $\Delta F = 100$ kHz.



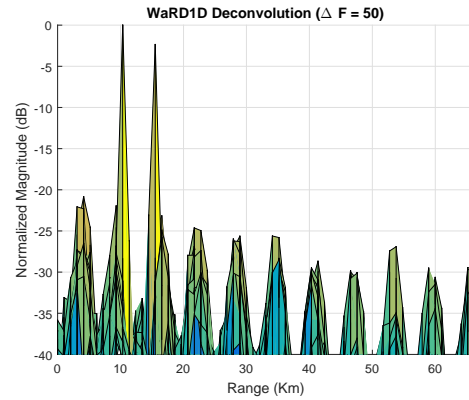
(a) Matched filter output of the scenario in Table 4.2 with $\Delta F = 50$ kHz.



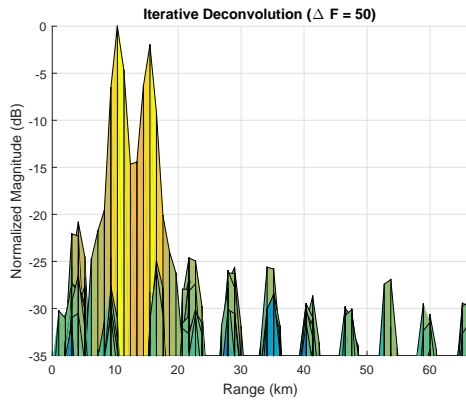
(b) Lucy-Richardson post processing of the matched filter output in Fig. 4.17a.



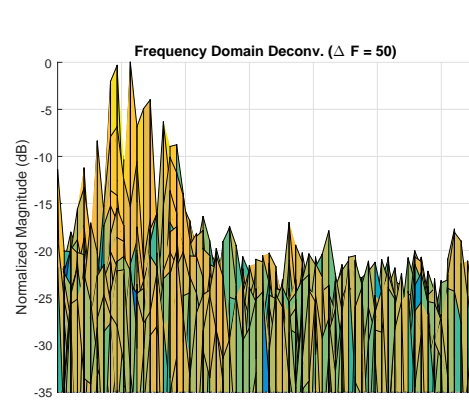
(c) DAMAS3 post processing of the matched filter output in Fig. 4.17a.



(d) WarD1D post processing of the matched filter output in Fig. 4.17a.



(e) Iterative Complex Deconv. post processing of the matched filter output in Fig. 4.14a.



(f) Frequency domain deconvolution.

Figure 4.17: Results of the third experiment with scenario in Table 4.2 and $\Delta F = 50$ kHz.

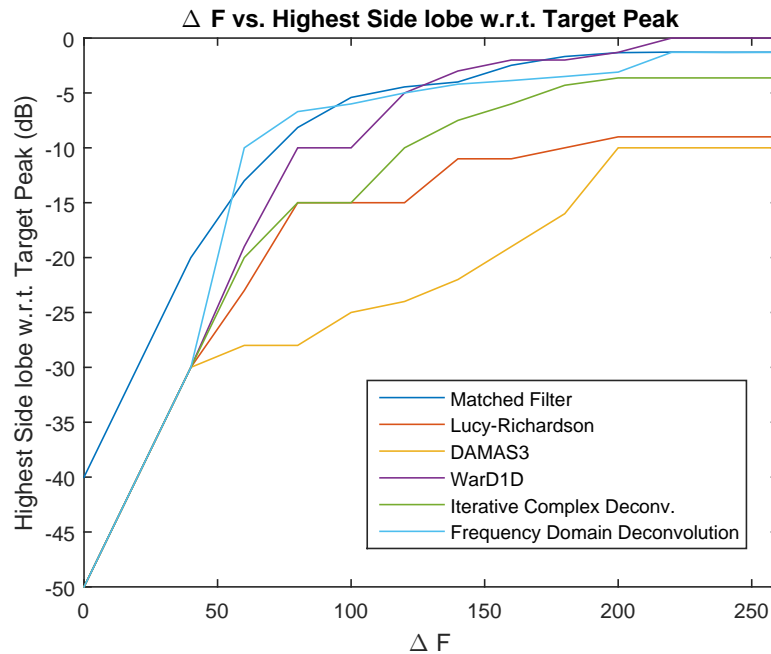


Figure 4.18: Comparison of matched filter and deconvolution post processing algorithms in the side lobe sense.

hand, was not successful on lowering the side lobe level. In the $\Delta F = 150$ kHz case, Lucy-Richardson and DAMAS3 algorithms managed to suppress the side lobes down to -10 and -22 dB respectively. Ward1D algorithm was able to also suppress the side lobes of the target at 10 km down to -20 dB, however, was not successful on dealing with the second target. Other 1-D deconvolution scheme, Iterative Complex Deconvolution, was successful on both lowering the side lobe and separating the second target. In the $\Delta F = 100$ kHz and $\Delta F = 50$ kHz cases, all algorithms were successful on suppressing the side lobe level effectively and revealed the actual target peaks. A similar graph for the overall performance of the deconvolution algorithm is in Fig. 4.18.

From Fig. 4.18, all deconvolution algorithms perform better compared to the matched filter in the side lobe sense except the 1-D deconvolution algorithm, WarD1D. Thus, it can be safely said that, deconvolution post processing is an effective tool for suppressing the side lobes that occur at the output of the matched

filter. In addition to this, time domain deconvolution schemes perform significantly better compared to the frequency domain deconvolution algorithm presented in [8].

A processing time comparison of the algorithms is in Table 4.3. The 2-D algorithms are run across the whole ambiguity function output where as it is possible to run the 1-D algorithms to just certain lines of the ambiguity function output. Since the ambiguity function is already computed, it is possible to only apply the 1-D deconvolution algorithms to certain Doppler shift lines that have target clusters. It is also possible to run 1-D algorithms in parallel as well since each Doppler line uses the same PSF and independent from each other. All algorithms are run on a system with i7-2.2 GHz processor, 8 GB RAM, 64-bit Windows 7 on Matlab. The ambiguity function outputs have 64 range bins and 64 Doppler bins. Processing times are average of 100 trails. The multichannel signal consists of three FM channels. In addition to this, iterative deconvolution algorithm iterates total of 10000 times. Other algorithms stop the iteration after the SNR is below a certain value.

Table 4.3: Processing time of the deconvolution algorithms and the matched filter.

PR system type	Algorithm	Processing time (seconds)
Single Channel	Matched Filter	1.89
Single Channel	Iterative Deconv.	0.34
Single Channel	WArD1D	0.19
Single Channel	Lucy-Richardson	0.22
Single Channel	DAMAS3	0.12
Multi Channel	Matched Filter	4.44
Multi Channel	Iterative Deconv.	0.37
Multi Channel	WArD1D	0.18
Multi Channel	Lucy-Richardson	0.21
Multi Channel	DAMAS3	0.13

Chapter 5

Conclusion

In this thesis, a novel post processing approach, that increases the overall target separation and range resolution of a FM based PR system is proposed. It is shown that the ambiguity function can be written as the convolution of a so called “channel impulse response” and the autocorrelation function of the transmitted signal. A typical PR system already computes the ambiguity function in order to generate the 2-D range-Doppler map. In addition to this, in order to compute the range-Doppler map, the transmitted signal is needed and is available to the PR system as well. Thus, it is shown that the channel impulse response that consists of impulses at the location of actual targets can be estimated using any non-blind deconvolution algorithm. In a PR system, the autocorrelation function of the transmitted signal is called the PSF, or the blurring function. In another sense, the channel impulse response is “blurred” or “spread” by the autocorrelation function of the transmitted signal.

It is experimentally shown that the deconvolution algorithms increase the overall target separation performance of the matched filter. For the single channel FM signals case, all of the deconvolution algorithms managed to significantly increase the target separation performance of the matched filter. For the multichannel FM signals case, the output of the matched filter is crowded by side lobes. These side lobes can be very high in amplitude that they might prevent the successful

detection of the actual target peaks. It is first experimentally shown that the separation between FM channels in frequency domain can be manipulated in order to lower the side lobe levels at the output of the matched filter. Then it is also shown that deconvolution can be used to further lower levels of the side lobes as well. In all separation between FM channels in frequency domain values, deconvolution post processing manages to perform better in the side lobe department compared to the matched filter.

Bibliography

- [1] H. Griffiths and C. Baker, “Passive coherent location radar systems. part 1: performance prediction,” in *Radar, Sonar and Navigation, IEE Proceedings-*, vol. 152, pp. 153–159, IET, 2005.
- [2] H. Kuschel and D. O’Hagan, “Passive radar from history to future,” in *Radar Symposium (IRS), 2010 11th International*, pp. 1–4, IEEE, 2010.
- [3] C. Baker, H. Griffiths, and I. Papoutsis, “Passive coherent location radar systems. part 2: Waveform properties,” *IEE Proceedings-Radar, Sonar and Navigation*, vol. 152, no. 3, pp. 160–168, 2005.
- [4] P. E. Howland, D. Maksimiuk, and G. Reitsma, “Fm radio based bistatic radar,” *IEE Proceedings-Radar, Sonar and Navigation*, vol. 152, no. 3, pp. 107–115, 2005.
- [5] “Radar.” <https://en.wikipedia.org/wiki/Radar>. Accessed: 2015-08-15.
- [6] M. A. Richards, *Fundamentals of radar signal processing*. Tata McGraw-Hill Education, 2005.
- [7] P. Bezoušek and V. Schejbal, “Bistatic and multistatic radar systems,” *Radioengineering*, vol. 17, no. 3, p. 53, 2008.
- [8] A. S. Tasdelen and H. Koymen, “Range resolution improvement in passive coherent location radar systems using multiple fm radio channels,” 2006.
- [9] A. Farina, R. Fulcoli, P. Genovesi, R. Lalli, R. Mancinelli, *et al.*, “Design, development and test on real data of an fm based prototypical passive radar,” in *Radar Conference, 2008. RADAR’08. IEEE*, pp. 1–6, IEEE, 2008.

- [10] R. I.-R. BS.450-3, “Bs.450 : Transmission standards for fm sound broadcasting at vhf,” 2001.
- [11] A. Lauri, F. Colone, R. Cardinali, C. Bongianni, and P. Lombardo, “Analysis and emulation of fm radio signals for passive radar,” in *Aerospace Conference, 2007 IEEE*, pp. 1–10, IEEE, 2007.
- [12] D. ETSI, “Radio broadcasting systems; digital audio broadcasting (dab) to mobile, portable and fixed receivers,” *Sophia Antipolis, France*, 2000.
- [13] C. Coleman and H. Yardley, “Dab based passive radar: performance calculations and trials,” in *International Conference on Radar (2008: Adelaide, Australia)*, 2008.
- [14] A. Capria, M. Conti, D. Petri, M. Martorella, F. Berizzi, E. Dalle Mese, R. Soleti, and V. Carulli, “Ship detection with dvb-t software defined passive radar,” in *IEEE Gold Remote Sensing Conference*, 2010.
- [15] K. E. Olsen, K. Woodbridge, I. Andersen, *et al.*, “Fm based passive bistatic radar target range improvement-part ii,” in *Radar Symposium (IRS), 2010 11th International*, pp. 1–8, IEEE, 2010.
- [16] D. O’Hagan, H. Kuschel, M. Ummenhofer, J. Heckenbach, and J. Schell, “A multi-frequency hybrid passive radar concept for medium range air surveillance,” *Aerospace and Electronic Systems Magazine, IEEE*, vol. 27, no. 10, pp. 6–15, 2012.
- [17] J.-J. Fuchs, “Multipath time-delay detection and estimation,” *Signal Processing, IEEE Transactions on*, vol. 47, no. 1, pp. 237–243, 1999.
- [18] M. Edrich, A. Schroeder, and V. Winkler, “Design and performance evaluation of a fm/dab/dvb-t multi-illuminator passive radar system,” 2012.
- [19] K. Olsen, “Fm-based passive bistatic radar as a function of available bandwidth,” Radar Conference, 2008. RADAR’08. IEEE, 2008.
- [20] A. K. Katsaggelos and R. W. Schafer, “Iterative deconvolution using several different distorted versions of an unknown signal,” in *Acoustics, Speech, and*

Signal Processing, IEEE International Conference on ICASSP'83., vol. 8, pp. 659–662, IEEE, 1983.

- [21] R. W. Schafer, R. M. Mersereau, M. Richards, *et al.*, “Constrained iterative restoration algorithms,” *Proceedings of the IEEE*, vol. 69, no. 4, pp. 432–450, 1981.
- [22] R. Neelamani, H. Choi, and R. Baraniuk, “Forward: Fourier-wavelet regularized deconvolution for ill-conditioned systems,” *Signal Processing, IEEE Transactions on*, vol. 52, no. 2, pp. 418–433, 2004.
- [23] W. H. Richardson, “Bayesian-based iterative method of image restoration,” *JOSA*, vol. 62, no. 1, pp. 55–59, 1972.
- [24] R. P. Dougherty, “Extensions of damas and benefits and limitations of deconvolution in beamforming,” *AIAA paper*, vol. 2961, no. 11, 2005.

Appendix A

Side-lobes and Multichannel Signals

Let us first consider two arbitrary, complex baseband, band-limited discrete signals $s_1[n]$ and $s_2[n]$ with bandwidths β_1 and β_2 respectively. Let:

$$s[n] = s_1[n] + s_2[n]e^{jw_2n}, \quad (\text{A.1})$$

where $w_2 \geq \beta_1 + \beta_2$ so that these two signals, $s_1[n]$ and $s_2[n]$, are rearranged in the frequency domain to generate the so called "multi-channel" signal. Let $c_s[k]$ be the autocorrelation sequence of $s[n]$:

$$c_s[k] = E\{s[n]s^*[n+k]\}, \quad (\text{A.2})$$

If we put $s[n] = s_1[n] + s_2[n]e^{jw_2n}$ in the expectation function $c_s[k]$ will be as follows:

$$\begin{aligned} c_s[k] &= E\{[s_1[n] + (s_2[n]e^{jw_2n})] \\ &\quad \times [s_1^*[n+k] + (s_2^*[n+k]e^{-jw_2(n+k)})]\} \end{aligned} \quad (\text{A.3})$$

Expanding the multiplication inside the summation and using the linearity of expectation operation we have:

$$\begin{aligned}
c_s[k] &= E\{s_1[n]s_1^*[n+k]\} \\
&+ E\{s_1[n](s_2^*[n+k]e^{-jw_2(n+k)})\} \\
&+ E\{(s_2[n]e^{jw_2n})s_1^*[n+k]\} \\
&+ E\{(s_2[n]e^{jw_2n})(s_2^*[n+k]e^{-jw_2(n+k)})\}
\end{aligned} \tag{A.4}$$

Which is the sum of four expectations. We can write $c_{s_i}[k]$ for $i = 1, 2, 3, 4$ as:

$$c_{s_1}[k] = E\{s_1[n]s_1^*[n+k]\} \tag{A.5a}$$

$$c_{s_1s_2}[k] = E\{s_1[n](s_2^*[n+k]e^{-jw_2(n+k)})\} \tag{A.5b}$$

$$c_{s_2s_1}[k] = E\{(s_2[n]e^{jw_2(n)})s_1^*[n+k]\} \tag{A.5c}$$

$$c_{s_2}[k] = E\{s_2[n]s_2^*[n+k]e^{-jw_2k}\} \tag{A.5d}$$

Here, we make a remark that sample autocorrelation sequence is defined for an arbitrary signal $x[n]$ as follows:

$$c_x[k] = \sum_{n=0}^{N-k-1} (x[n]x[n+k]), \tag{A.6}$$

and convolution of sequence $x[n]$ is defined as follows:

$$(x * x)[k] = \sum_{n=0}^{N-k-1} (x[n]x[k-n]). \tag{A.7}$$

Thus the convolution of sequence $x[n]$ with its time reversed self at k is defined also the autocorrelation of sequence $x[n]$ at k^{th} lag:

$$c_x[k] = x[-k] * x[k]. \tag{A.8}$$

Taking the Fourier transform,

$$C_x[w] = X[w]X[w]. \tag{A.9}$$

Correlation is equal to the multiplication in frequency domain. Now going back to the signal $s[n]$, we can write Eqs. A.5b and A.5c as follows:

$$C_{s_1s_2}[w] = S_1[w]S_2[w - w_2], \quad (\text{A.10a})$$

$$C_{s_2s_1}[w] = S_2[w - w_2]S_1[w], \quad (\text{A.10b})$$

where $C_{s_1s_2}[w]$ and $C_{s_2s_1}[w]$ are Fourier transforms of $c_{s_1s_2}[k]$ and $c_{s_2s_1}[k]$ respectively. Taking in to account that in these equations, $w_2 \geq \beta_1 + \beta_2$, these multiplications will yield 0 and Eq. A.4 can be written as follows:

$$c_s[k] \approx c_{s_1}[k] + c_{s_2}[k] \quad (\text{A.11})$$

where $c_{s_2}[k]$ is a modulated expectation such that:

$$c_{s_2}[k] = E\{s_2[n]s_2^*[n+k]\}e^{-jw_2k} \quad (\text{A.12})$$

Summing $c_{s_1}[k]$ and $c_{s_2}[k]$ will result with a modulated $c_s[k]$ as well which creates the "side lobes" in the autocorrelation function.

Expanding the correlation function to $s[n] = s_1[n] + s_2[n]e^{jw_2n} + s_3[n]e^{jw_3n}$ will have a similar result:

$$c_s[k] \approx c_{s_1}[k] + c_{s_2}[k] + c_{s_3}[k] \quad (\text{A.13})$$

Lastly, we can generalize the expectation function for $s[n] = s_1[n] + s_2[n]e^{jw_2n} + \dots + s_L[n]e^{jw_Ln}$ as:

$$c_s[k] \approx c_{s_1}[k] + c_{s_2}[k] + \dots + c_{s_L}[k] \quad (\text{A.14})$$

where $l = 1, 3, \dots, L$ for expectation of sum of L signals. The multichannel signal approach results in a modulated autocorrelation function independent of the signal.

Appendix B

DAMAS3 Deconvolution Algorithm

The Deconvolution Approach for the Mapping of Acoustic Sources (DAMAS) algorithm is a family of deconvolution algorithms. It was used in phased array acoustic arrays. Since the original algorithm is based on Wiener filtering is too slow and lacks regularization of noise amplification, two extensions, DAMAS2 and DAMAS3 are proposed. In the DAMAS2 algorithm, regularization is applied by a low pass filter and the algorithm is applied faster than the original DAMAS. In the DAMAS3, the speed of the algorithm is further increased and the regularization is applied using a Wiener filter. In DAMAS2 and DAMAS3 algorithms, the PSF is restricted such that it is in a convolutional form.

Let $p(\mathbf{x}, \mathbf{x}')$ be a point spread function that connects a source at \mathbf{x}' to an image at \mathbf{x} and if the actual distribution of the source phase array is $q(\mathbf{x})$. Then the observed signal is [24]:

$$b(\mathbf{x}) = \int p(\mathbf{x}, \mathbf{x}')q(\mathbf{x}')d\mathbf{x}'. \quad (\text{B.1})$$

Ideally, the PSF should be equal to $\delta(\mathbf{x} - \mathbf{x}')$. This means that Eq. B.1 is a source strength distribution, thus a convolutional operation and can be re-expressed as

follows:

$$b(\mathbf{x}) = \int p(\mathbf{x} - \mathbf{x}')q(\mathbf{x}')d\mathbf{x}'. \quad (\text{B.2})$$

Hence, if the PSF is known, it is possible to solve $q(\mathbf{x}')$ using deconvolution. In original DAMAS algorithm, Eq. B.1 is considered as a Fredholm integral of the first kind for $q(\mathbf{x})$. In a typical approach, $b(\mathbf{x})$ is measured on a grid and $q(\mathbf{x})$ is considered as the unknown actual distribution of the grid. Then the deconvolution boils down to the following linear algebra problem,

$$\mathbf{y} = \mathbf{A}\mathbf{x}, \quad (\text{B.3})$$

where \mathbf{y} is the measurement vector obtained by stacking $b(\mathbf{x})$, \mathbf{x} is the measurement vector of actual beamforming map obtained by stacking $q(\mathbf{x})$ and \mathbf{A} is the becomes the PSF. Thus, for known PSF, \mathbf{x} can be solved. In our case, typical size of the map is 100x100, which results in a possible A matrix with size 10000x10000. This results in a slow processing speed due to the large sizes of the matrices. In addition to this, during the deconvolution algorithm, well known Wiener filter approach is employed as follows:

Algorithm 2: Wiener filter deconvolution.

Input: $b(\mathbf{x}), p(\mathbf{x})$

Output: $q(\mathbf{x})$

- 1 Compute the FFT of inputs, $b(\mathbf{x}), p(\mathbf{x})$,
 - 2 For each frequency \mathbf{f} , $q(\mathbf{f}) = \frac{p^*(\mathbf{f})b(\mathbf{f})}{p^*(\mathbf{f})p(\mathbf{f})+\gamma}$
 - 3 Compute the IFFT of $q(\mathbf{f})$ to obtain $q(\mathbf{x})$.
-

In Algorithm 2, γ is used to avoid division by zero and * denotes complex conjugation. Original DAMAS is very sensitive to noise since it does not employ a noise regularization.

In DAMAS2, noise regularization is added and the speed of the algorithm improved using a FFT, frequency-by-frequency multiplication and IFFT approach respectively. The algorithm is as follows:

Algorithm 3: DAMAS2 deconvolution.

Input: $b(\mathbf{x}), p(\mathbf{x})$ **Output:** $q(\mathbf{x})$

- 1 Compute the FFT, $pt(\mathbf{f}) = F\{p(\mathbf{x})\}$,
 - 2 Set $a = \sum |p(\mathbf{x})|$,
 - 3 Set $q(\mathbf{x}) = 0$,
 - 4 Compute $q(\mathbf{f}) = FFT\{q(\mathbf{x})\}$,
 - 5 For each frequency \mathbf{f} , compute $\hat{q}(\mathbf{f}) = q(\mathbf{f})e^{-f^2/(2k_c^2)}$,
 - 6 Compute $r(\mathbf{f}) = p(\mathbf{f})\hat{q}(\mathbf{f})$,
 - 7 Compute $r(\mathbf{x}) = F^{-1}\{r(\mathbf{f})\}$,
 - 8 Set $q(\mathbf{x}) \leftarrow q(\mathbf{x}) + \frac{b(\mathbf{x})-r(\mathbf{x})}{a}$ for each \mathbf{x} ,
 - 9 Repeat from 4.
-

In Algorithm 3, k_c is the variance parameter of the Gaussian low-pass filter based regularization. DAMAS2 algorithm is much faster and more robust against noise.

In DAMAS3, the hybrid of DAMAS2 and Wiener deconvolution is employed. In the algorithm, original deconvolution problem, $b = p * q$ is modified using Wiener division and $b_w = p_w * q$ is obtained. The algorithm is as follows [24]:

Algorithm 4: DAMAS3 deconvolution.

Input: $b(\mathbf{x}), p(\mathbf{x})$ **Output:** $q(\mathbf{x})$

- 1 Compute the FFT of inputs, $b(\mathbf{x}), p(\mathbf{x})$,
 - 2 For each frequency \mathbf{f} , $b_w(\mathbf{f}) = \frac{p^*(\mathbf{f})b(\mathbf{f})}{p^*(\mathbf{f})p(\mathbf{f})+\gamma}$ and $p_w(\mathbf{f}) = \frac{p^*(\mathbf{f})p(\mathbf{f})}{p^*(\mathbf{f})p(\mathbf{f})+\gamma}$
 - 3 Compute the IFFT of $p_w(\mathbf{f})$ to obtain $p_w(\mathbf{x})$,
 - 4 Set $a = \sum |p_w(\mathbf{x})|$,
 - 5 Set $q(\mathbf{x}) = 0$,
 - 6 Compute $q(\mathbf{f}) = FFT\{q(\mathbf{x})\}$,
 - 7 Compute $r(\mathbf{f}) = p_w(\mathbf{f})q(\mathbf{f})$,
 - 8 Compute $r(\mathbf{x}) = F^{-1}\{r(\mathbf{f})\}$,
 - 9 Set $q(\mathbf{x}) \leftarrow q(\mathbf{x}) + \frac{b_w(\mathbf{x})-r(\mathbf{x})}{a}$ for each \mathbf{x} ,
 - 10 Repeat from 6.
-

In DAMAS3 algorithm, filtering that is used in step 5 of DAMAS2 algorithm is not needed and the Wiener filtering reduces the number of iterations needed greatly, resulting in even faster convergence compared to DAMAS2 [24].